RESEARCH ARTICLE

Modular mimicry and engagement of the Hippo pathway by Marburg virus VP40: Implications for filovirus biology and budding

Ziying Han[1], Shantoshini Dash[1], Cari A. Sagum[2], Gordon Ruthel[1], Chaitanya K. Jaladanki[3], Corbett T. Berry[1], Michael P. Schwoerer[1], Nina M. Harty[1], Bruce D. Freedman[1], Mark T. Bedford[2], Hao Fan[3], Sachdev S. Sidhu[4], Marius Sudol[3], Olena Shtanko[5], Ronald N. Harty[1]*

1 Department of Pathobiology, School of Veterinary Medicine, University of Pennsylvania, Philadelphia, Pennsylvania, United States of America, 2 Department of Epigenetics & Molecular Carcinogenesis, M.D. Anderson Cancer Center, University of Texas, Smithville, Texas, United States of America, 3 Department of Physiology and Mechanobiology Institute at National University of Singapore, Institute for Molecular and Cell Biology, IMCB, and Bioinformatics Institute, Agency for Science, Technology and Research (A*STAR), Singapore, 4 Department of Molecular Genetics, University of Toronto, Toronto, Ontario, Canada, 5 Texas Biomedical Research Institute, San Antonio, Texas, United States of America

* rharty@vet.upenn.edu

Abstract

Ebola (EBOV) and Marburg (MARV) are members of the *Filoviridae* family, which continue to emerge and cause sporadic outbreaks of hemorrhagic fever with high mortality rates. Filoviruses utilize their VP40 matrix protein to drive virion assembly and budding, in part, by recruitment of specific WW-domain-bearing host proteins *via* its conserved PPxY Late (L) domain motif. Here, we screened an array of 115 mammalian, bacterially expressed and purified WW-domains using a PPxY-containing peptide from MARV VP40 (mVP40) to identify novel host interactors. Using this unbiased approach, we identified Yes Associated Protein (YAP) and Transcriptional co-Activator with PDZ-binding motif (TAZ) as novel mVP40 PPxY interactors. YAP and TAZ function as downstream transcriptional effectors of the Hippo signaling pathway that regulates cell proliferation, migration and apoptosis. We demonstrate that ectopic expression of YAP or TAZ along with mVP40 leads to significant inhibition of budding of mVP40 VLPs in a WW-domain/PPxY dependent manner. Moreover, YAP colocalized with mVP40 in the cytoplasm, and inhibition of mVP40 VLP budding was more pronounced when YAP was localized predominantly in the cytoplasm rather than in the nucleus. A key regulator of YAP nuclear/cytoplasmic localization and function is angiomotin (Amot); a multi-PPxY containing protein that strongly interacts with YAP WW-domains. Interestingly, we found that expression of PPxY-containing Amot rescued mVP40 VLP egress from either YAP- or TAZ-mediated inhibition in a PPxY-dependent manner. Importantly, using a stable Amot-knockdown cell line, we found that expression of Amot was critical for efficient egress of mVP40 VLPs as well as egress and spread of authentic MARV in infected cell cultures. In sum, we identified novel negative (YAP/TAZ) and positive (Amot) regulators of MARV VP40-mediated egress, that likely function in part, via competition between host and viral PPxY motifs binding to modular host WW-domains. These findings

Competing interests: The authors have declared that no competing interests exist.

not only impact our mechanistic understanding of virus budding and spread, but also may impact the development of new antiviral strategies.

Author summary

By screening an array of 115 mammalian WW-domains with the PPxY motif from MARV VP40 (mVP40), we identified YAP1 and TAZ, transcriptional effectors of the Hippo pathway, as mVP40 interactors, and demonstrated that ectopically expressed YAP1 or TAZ inhibited budding of mVP40 virus-like particles (VLPs) in a WW-domain/PPxY dependent manner. Angiomotin (Amot), a multi-PPxY containing regulator of YAP1 nuclear/cytoplasmic localization and function, rescued mVP40 VLP egress from either YAP1- or TAZ-mediated inhibition in a PPxY-dependent manner. Indeed, endogenous Amot expression was critical for egress of mVP40 VLPs and authentic MARV. In sum, we have revealed a link between the Hippo pathway and filovirus egress by identifying negative (YAP/TAZ) and positive (Amot) regulators of MARV VP40-mediated egress.

Introduction

Filoviruses (Ebola [EBOV] and Marburg [MARV]) are high-priority, emerging pathogens, for which there are no approved vaccines nor therapeutic agents. As EBOV and MARV have been reported to cross epithelial and endothelial cell barriers and re-emerge months later in immunologically privileged sites including the CNS, semen, and retina, a better understanding of viral-host interactions that contribute to the transmission and pathogenesis of these deadly viruses is more critical than ever [1–4]. VP40 is the major structural protein that uniquely and independently directs assembly and egress of both virus-like particles (VLPs) and infectious filovirus virions. To accomplish this, VP40 uses highly conserved Late (L) budding domains (L-domains) that function to recruit or hijack a select set of host proteins that facilitate late stages of virus-cell separation [5–13]. For example, the well-described PPxY L-domain motif mediates the recruitment of a series of host HECT-family E3 ubiquitin ligases *via* one or more of their cognate WW-domains to facilitate egress [9,10,14–20]. In general, viral PPxY/WW-domain interactions involving host E3 ligases are believed to promote mono-ubiquitinylation of the viral matrix proteins [11–13,21–39], which allows the viral matrix protein to engage the ESCRT machinery to facilitate virus-cell separation at the plasma membrane [5,7,11–13,21,23–27,31,35–45].

There is a built-in degree of specificity of PPxY/WW-domain binding such that specific PPxY containing proteins will only interact physically and functionally with select WW-domain partners [46–49]. To date, much of the focus on viral L-domain motifs has been on their recruitment of host E3 ubiquitin ligases and/or the ESCRT pathway to advance virus egress and spread. To identify other cellular pathways employing WW-domain bearing proteins that could potentially affect filovirus egress and spread, and to further identify the overall complement of WW domains and its host proteins capable of binding to filovirus VP40 PPxY motifs, we probed a GST-fused array of 115 mammalian WW domains that were bacterially expressed, purified and fixed on solid support [50] with WT or mutant PPxY containing peptides from mVP40. Results from our screen identified two novel mVP40 PPxY interactors; YAP (Yes Associated Protein) and TAZ (Transcriptional co-Activator with PDZ-binding motif, also known as WWTR1 [WW domain-containing Transcription Regulator 1]).

YAP/TAZ are functional paralogues and the final downstream transcriptional effectors of the Hippo signaling pathway that regulates organ development, cell proliferation, migration, survival, and homeostasis [51–57]. Intriguingly, the Hippo signaling pathway is regulated by a series of PPxY/WW-domain modular interactions which lead ultimately to either sequestration or degradation of phosphorylated YAP in the cytoplasm (Hippo on), or to localization of unphosphorylated YAP in the nucleus where it upregulates a series of TEAD genes involved in cell growth and proliferation (Hippo off) [58]. One of the key regulators of YAP/TAZ localization and Hippo pathway activity is angiomotin (Amot), a member of the angiomotin family (Amot, AmotL1, and AmotL2), all of which contain multiple PPxY motifs at their N-termini [59–65]. Indeed, the PPxY/WW-domain interaction between Amot and YAP is well-characterized and reported to affect multiple processes in the cell [60–62,64–69].

In this report, we sought to determine whether the PPxY/WW-domain interaction between mVP40 and YAP/TAZ affected mVP40-mediated budding, and whether the PPxY motifs of Amot could compete with mVP40 for YAP1 binding to diminish these effects. Indeed, we found that: 1) co-expression of YAP1 or TAZ with mVP40 inhibited egress of mVP40 VLPs, 2) mVP40 VLP egress was not inhibited as significantly by YAP1 localized predominantly in the nucleus, 3) Amot expression positively regulated mVP40 VLP budding and rescued budding of mVP40 VLPs in the presence of YAP1 in a PPxY-dependent manner, and 4) Amot expression enhanced release and spread of authentic MARV in cell culture. These findings provide evidence that both PPxY and WW-domain proteins of the Hippo signaling pathway act as novel interactors and/or regulators of MARV VP40-mediated egress and spread. Moreover, these results highlight the potential domain mimicry and competitive interplay between host and viral proteins that can result in either a favorable or unfavorable outcome for the virus. The consequences of this intersection between virus budding and Hippo signaling not only may impact virus egress and spread, but also influence the biology and pathogenesis of filoviruses.

Results

Identification of YAP and TAZ as WW-domain interactors with the PPxY motif of mVP40

We used fluorescently-labeled, biotinylated peptides containing WT or mutated PPxY motifs from mVP40 to screen an array composed of 115 WW-domains and 40 SH3-domains that are derived from human proteins to detect novel host interactors (Fig 1A). We identified a select number of host WW-domain interactors (see Supplementary S1 Table) using the WT mVP40 peptide, whereas the mVP40 PPxY mutant peptide did not interact with any WW- or SH3-domain on the array (Fig 1A). Among the interactors identified were several HECT family E3 ubiquitin ligases that we and others have identified previously, as well as two novel WW-domain interactors; YAP1 and TAZ (Fig 1A and 1B).

There are two major isoforms of YAP; YAP1-1 contains one WW-domain (WW1), whereas YAP1-2 contains two WW-domains (WW1 and WW2) [70]. To validate further the interaction between the mVP40 PPxY motif and the WW-domains of YAP and TAZ, we used GST-YAP-WW1, GST-YAP-WW2, and GST-TAZ-WW fusion proteins to pulldown full-length mVP40-WT or mVP40-PYA4 mutant proteins expressed in HEK293T cells (Fig 1C and 1D). We found that mVP40-WT interacted strongly with WW1 of YAP1 (Fig 1C, lane 3), and weakly with WW2 of YAP1-2 (Fig 1C, lane 4). mVP40-PYA4 did not interact with either YAP WW1 or WW2 domains (Fig 1C, lanes 5 + 6). Similarly, we found that mVP40-WT, but not mVP40-PYA4, interacted with GST-TAZ-WW (Fig 1D, lanes 2 + 3). Consistent levels of expression for all GST fusion proteins (Fig 1C, lanes 1–6, and Fig 1D, lanes 1–3; anti-GST),
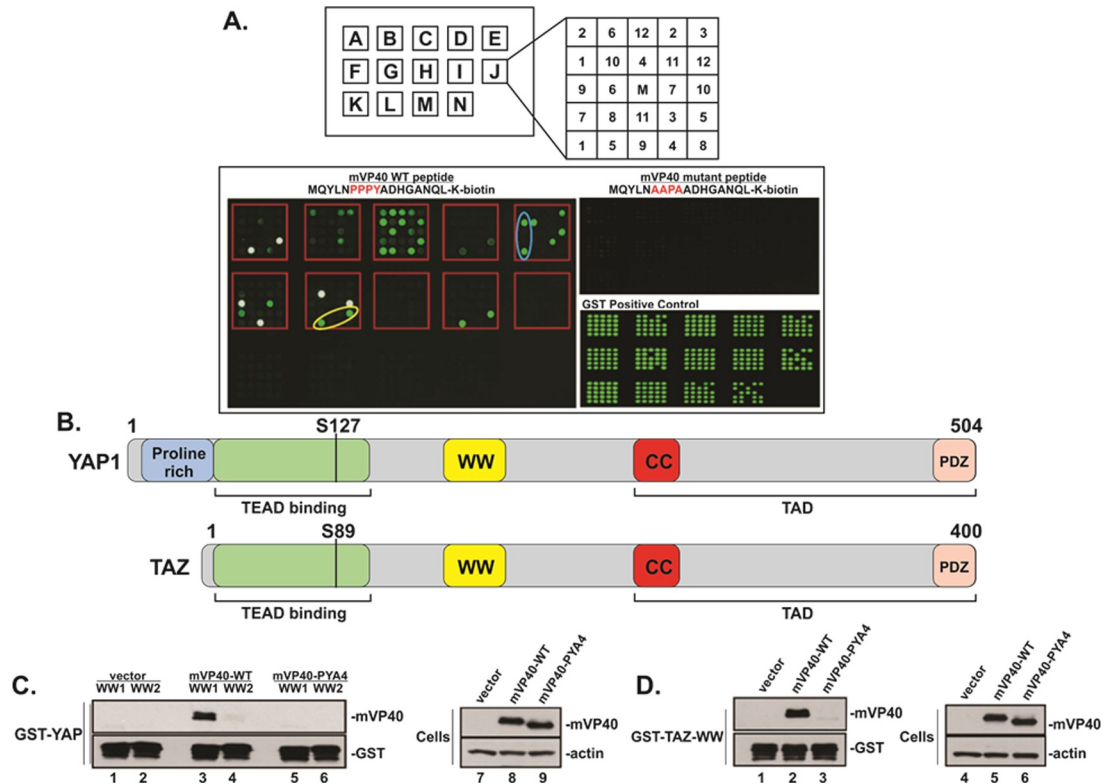
Fig 1. Screening array of modular proteins and GST-pulldown assays. A) Twelve different GST-SH3 and GST-WW domain fusion proteins per lettered box were arrayed in duplicate as indicated in enlarged box J (Top). The center sample (M) in each box represents GST alone as a negative control. The array was screened with biotinylated PPxY-WT or PPxY-mutant peptides of MARV VP40. Representative data for mVP40-WT peptide (MQYLN**PPPY**ADHGANQL-[Lys-Biotin]) (50µg), and mVP40-mutant peptide (MQYLN<u>AAPA</u>ADHGANQL-[Lys-Biotin]) (50µg) are shown. The mVP40-mutant peptide did not interact with any GST-SH3 or GST-WW domain fusion protein (center), whereas the mVP40-WT peptide interacted with specific GST-WW domain fusion proteins, including YAP1-1-WW (blue oval) and TAZ-WW (yellow oval). A positive control for expression of all GST-WW fusion proteins is shown. **B)** Schematic diagrams of human YAP1 and TAZ with key domains highlighted are shown. Numbers represent amino acids. Serine 127 and serine 89 are key sites for phosphorylation. TEAD = TEA DNA binding domain; WW = WW domain, CC = coiled coil domain; TAD = transcriptional activation domain; PDZ = PSD-95/Dlg1/ZO-1 domain. **C)** Input levels of purified GST-YAP-WW1 and GST-YAP-WW2 fusion proteins were shown to be consistent for all samples as determined by Western blotting using anti-GST antiserum (lanes 1–6). Only mVP40-WT was pulled down by GST-YAP-WW1 (lane 3). Expression levels for mVP40-WT, mVP40-PYA4, and actin in transfected HEK293T cells are shown (lanes 7–8). **D)** Input levels of purified GST-TAZ-WW fusion protein were shown to be consistent for all samples as determined by Western blotting using anti-GST antiserum (lanes 1–3). Only mVP40-WT was pulled down by GST-TAZ-WW (lane 2). Expression levels for mVP40-WT, mVP40-PYA4, and actin in transfected HEK293T cells are shown (lanes 4–6).

https://doi.org/10.1371/journal.ppat.1008231.g001

mVP40-WT (Fig 1C, lane 8 and Fig 1D, lane 5), and mVP40-PYA4 (Fig 1C, lane 9 and Fig 1D, lane 6) were confirmed by Western blotting. Taken together, these data indicate that the PPxY motif of mVP40 can interact specifically and robustly with YAP-WW1 and TAZ-WW domains.

Ectopic Expression of YAP1 or TAZ inhibits mVP40 VLP budding

Next, we sought to determine whether exogenous expression of either YAP1 or TAZ with mVP40 would affect egress of mVP40 VLPs. Briefly, mVP40-WT or budding defective mutant mVP40-PYA4 were co-expressed with YAP1 WT or a mutant lacking the WW-domain (YAP1 mut) in HEK293T cells, and both cell extracts and VLPs were harvested at 24 hours post-transfection and analyzed by Western blotting (Fig 2A). When equal amounts of mVP40-WT and
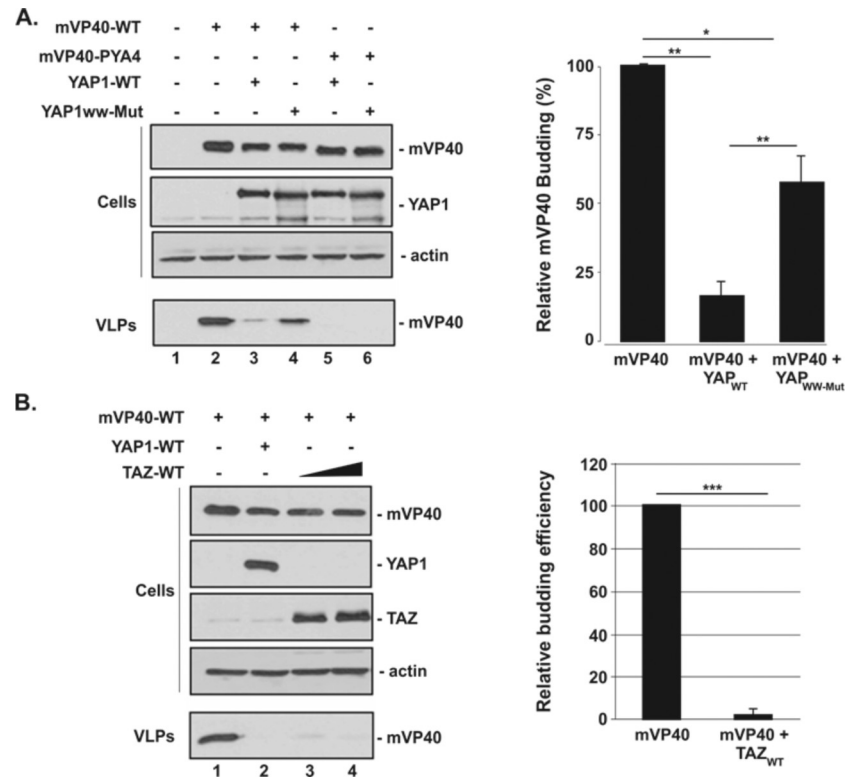
Fig 2. mVP40 VLP budding assay with YAP or TAZ. A + B) Budding of mVP40 VLPs was assessed from cells co-expressing WT or mutant forms of YAP or TAZ. HEK293T cells were transfected with the indicated combinations of plasmids (0.5µg/each for panel A, 0.25µg of mVP40-WT, YAP1-WT, and 0.25µg and 0.5µg of TAZ-WT for panel B), and both cell extracts and VLPs were harvested at 24 hrs post-transfection. The indicated proteins were detected and quantified in cells and VLPs by Western blotting and NIH Image-J, respectively. Bar graphs represent data from at least three independent experiments, and samples were compared using Welch's t-test. * $p<0.05$, ** $p<0.01$, *** $p<0.001$.

YAP1 WT plasmids were co-transfected, we observed a consistent and significant decrease in mVP40 VLP egress (Fig 2A, compare lanes 2 + 3). Interestingly, co-expression of mVP40 with the YAP1 WW domain mutant did not yield the same level of VLP inhibition (Fig 2A, compare lanes 2 + 4). As expected, the mVP40-PYA4 mutant was defective in its ability to bud on its own, and thus there was no observed effect of YAP1 WT or mutant proteins on egress of mVP40-PYA4 (Fig 2A, lanes 5 + 6). Likewise, we observed a similar inhibitory effect on mVP40 VLP egress when TAZ-WT was co-expressed with mVP40 (Fig 2B). Together, these data show that either YAP1 or TAZ expression lead to inhibition of mVP40 VLP egress, which likely occurs in a WW-domain dependent manner.

YAP1 overlaps with mVP40 in the cytoplasm and sequesters mVP40 away from the plasma membrane

We used confocal microscopy to determine whether YAP1 WT or YAP1 WW-domain mutant exhibited a similar localization pattern with mVP40 in HEK293T cells. As expected, expression of mVP40 alone resulted in abundant localization at the cell surface and its appearance in membrane projections was indicative of efficient VLP egress (Fig 3, mVP40). Ectopic expression of YAP1 alone revealed a mainly cytoplasmic pattern of localization (Fig 3, YAP1 WT). When co-expressed, mVP40 overlapped with YAP1 WT in punctate aggregates in the
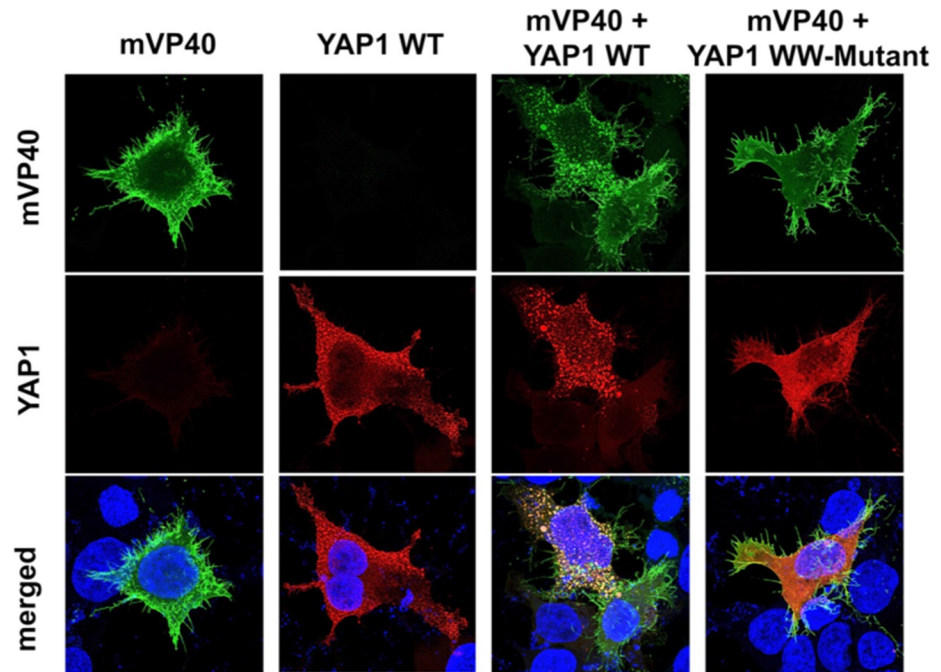
**Fig 3. Intracellular localization of mVP40 and YAP.** HEK293T cells were transfected with YFP-mVP40 alone, CFP-YAP1 WT alone, YFP-mVP40 + CFP-YAP1 WT, or YFP-mVP40 + CFP-YAP1 WW mutant (0.25μg/each). Confocal images for each condition are shown with mVP40 in green, YAP in red, and nuclei in blue. Overlap of YFP-mVP40 and CFP-YAP WT is indicated by yellow fluorescence in merged images. Scale bars = 10μm.

https://doi.org/10.1371/journal.ppat.1008231.g003

cytoplasm and the appearance of membrane projections was greatly reduced (Fig 3, mVP40 + YAP1 WT). Interestingly, YAP1 WW-domain mutant did not overlap significantly with mVP40, and the mVP40 membrane projections remained prominent in these cells (Fig 3, mVP40 + YAP1 WW-mutant). Together, these data correlate well with VLP budding data above to suggest that ectopically expressed YAP1 interacts with mVP40 in the cytoplasm in a PPxY/WW-domain dependent manner to inhibit VLP egress, potentially by sequestering mVP40 away from the site of budding at the plasma membrane.

Inhibition of mVP40 VLP egress is rescued by nuclear localization of YAP1

The function of YAP1 as a transcriptional effector of the Hippo pathway is dependent on its phosphorylation state, which dictates its ability to either enter the nucleus (unphosphorylated) or remain sequestered in the cytoplasm (phosphorylated) [71]. Therefore, we next sought to determine whether the predominantly nuclear localization of exogenously expressed YAP1 would reduce its availability to interact directly with mVP40 resulting in an increase in VLP egress. Toward this end, we ectopically expressed YAP1-S127A, a well characterized, transcriptionally active mutant that is not phosphorylated on Serine127 and thus localizes predominantly to the nucleus [72,73]. Briefly, HEK293T cells were transfected with mVP40 alone, mVP40 plus YAP1 WT, or mVP40 + YAP1 S127A, and both cell extracts and VLPs were harvested and analyzed by Western blotting (Fig 4). As described above, expression of YAP1 WT resulted in inhibition of mVP40 VLP egress; however, the degree of inhibition was significantly reduced in the presence of mutant YAP1 S127A in repeated experiments (Fig 4, compare lanes 2 + 3). These results suggest that when YAP1 is largely in the cytoplasm, its ability to
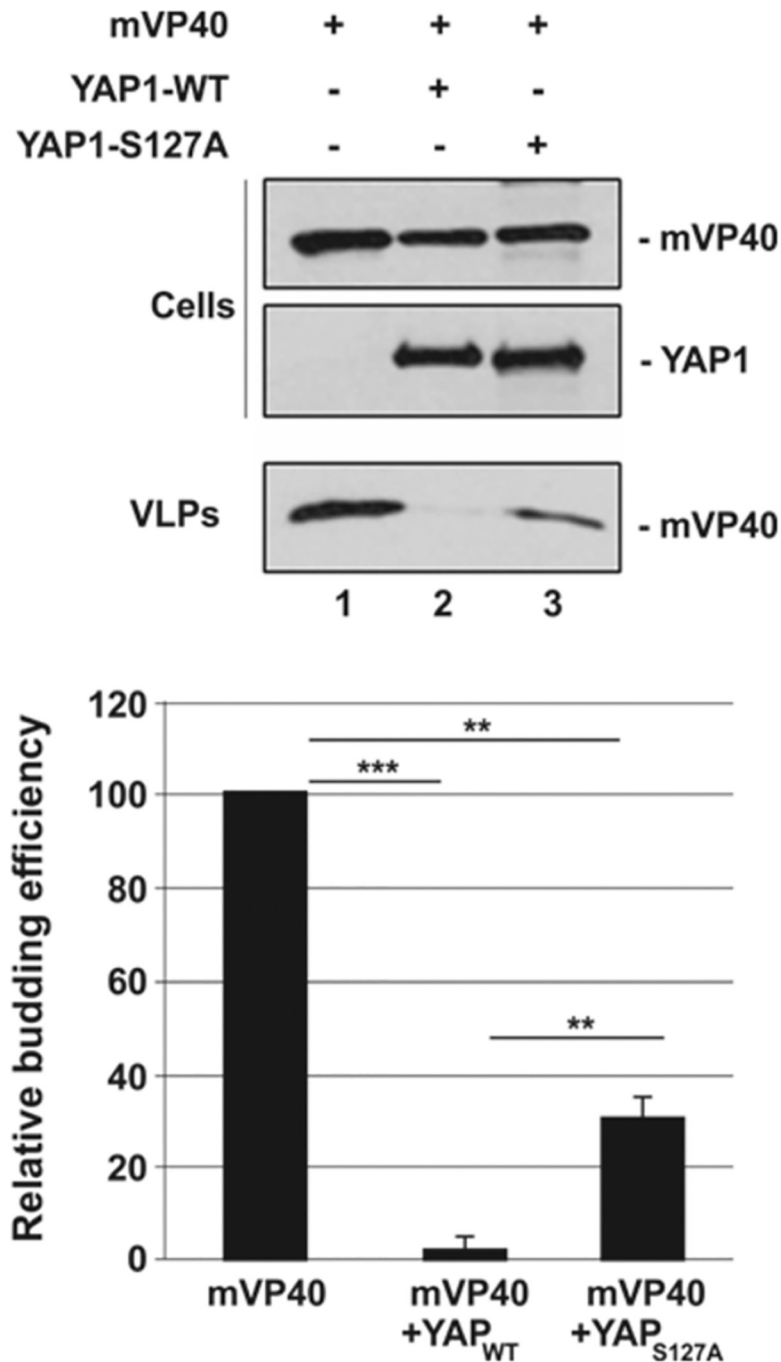
Fig 4. mVP40 VLP budding assay with WT and mutant YAP1. HEK293T cells were transfected with the indicated combinations of plasmids (0.25μg of mVP40 and 0.5μg of YAP plasmids), and both cell extracts and VLPs were harvested at 24 hrs post-transfection. The YAP1 S127A mutant cannot be phosphorylated at this position and is predominantly found in the nucleus. The indicated proteins were detected and quantified in cells and VLPs by Western blotting and NIH Image-J, respectively. Bar graphs represent data from at least three independent experiments. ** $p < 0.01$, *** $p < 0.001$.

https://doi.org/10.1371/journal.ppat.1008231.g004

engage mVP40 results in inhibition of VLP egress, whereas when YAP1 is predominantly in the nucleus, it cannot engage mVP40 as efficiently and thus has less of an impact on VLP egress.
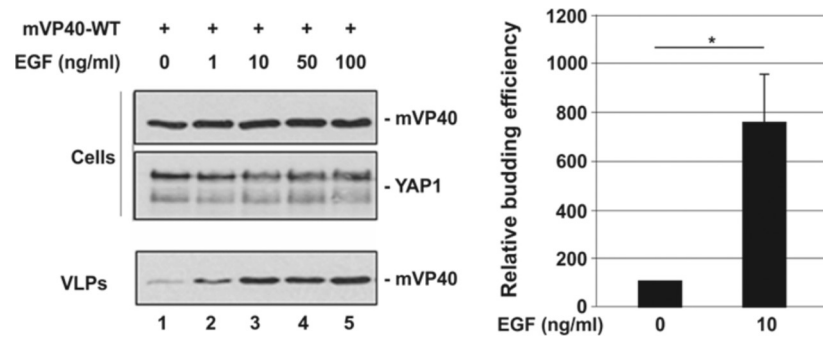
Fig 5. Activation of the Endogenous Hippo pathway impacts mVP40 VLP budding. U2OS cells were transfected with mVP40-WT (2μg) for 24 hrs, and then stimulated for an additional 24 hrs with the indicated concentration of purified EGF. The indicated proteins were detected and quantified in cells and VLPs by Western blotting and NIH Image-J, respectively. The bar graph represents data from three independent experiments of cells stimulated with either 0 or 10 ng/ml of EGF. The relative budding efficiency of mVP40 peaked at 10ng/ml of EGF with an average increase of approximately 7.5-fold vs. control. * p = 0.03 as determined by Welch's t-test.

Budding of mVP40 VLPs is enhanced in the context of endogenous Hippo pathway activation

We next sought to determine whether mVP40 VLP budding would be impacted following activation of the endogenous Hippo pathway by treating mVP40-expressing cells with epidermal growth factor (EGF). Briefly, U2OS cells were first transfected overnight with mVP40-WT, and then treated with increasing amounts of EGF, which has been shown to trigger translocation of endogenous YAP into the nucleus [74]. We observed a dose-dependent and significant increase (up to 7.5-fold) in mVP40 VLP egress in the presence of increasing concentrations of EGF (Fig 5, lanes 1–5). Cellular levels of mVP40 and endogenous YAP1 were found to be equivalent in all samples (Fig 5, lanes 1–5). These results are consistent with those shown in Fig 4 and suggest that endogenous Hippo pathway activation regulates mVP40-mediated egress.

Budding of mVP40 VLPs occurs efficiently in YAP knockout (KO) cells

To further validate the role of YAP as a potential regulator of mVP40 VLP egress, we used an HEK293-based YAP KO cell line [75]. Briefly, YAP KO cells were transfected with either mVP40 alone or mVP40 + YAP1 WT, and both cell extracts and VLPs were harvested and analyzed by Western blotting (Fig 6). We observed efficient egress of mVP40 VLPs from the YAP KO cells; however, mVP40 VLP egress was significantly inhibited when the YAP KO cells were spiked with exogenous YAP1 WT (Fig 6). These results are consistent with those described above, and taken together, the results shown in Figs 2–6 suggest that YAP/TAZ and the Hippo pathway have a functional impact on mVP40-mediated budding.

mVP40 VLP budding is inhibited in shAmot knockdown cells

Human angiomotin (Amot-p130) contains multiple PPxY motifs at its N-terminus and is a well-characterized, strong interactor and regulator of YAP1 localization and activity, whereas Amot-p80 is an N-terminally truncated mutant lacking all PPxY motifs (Fig 7A) [61,63–65,69,76,77]. This prompted us to ask whether Amot expression would have an effect on mVP40 VLP egress. We used an HEK293T-based cell line stably expressing a lentiviral short hairpin RNA specific for Amot (shAmot) to assess egress of mVP40 VLPs compared to that from Amot expressing control cells (shCtrl) [64]. Briefly, shCtrl or shAmot cells were
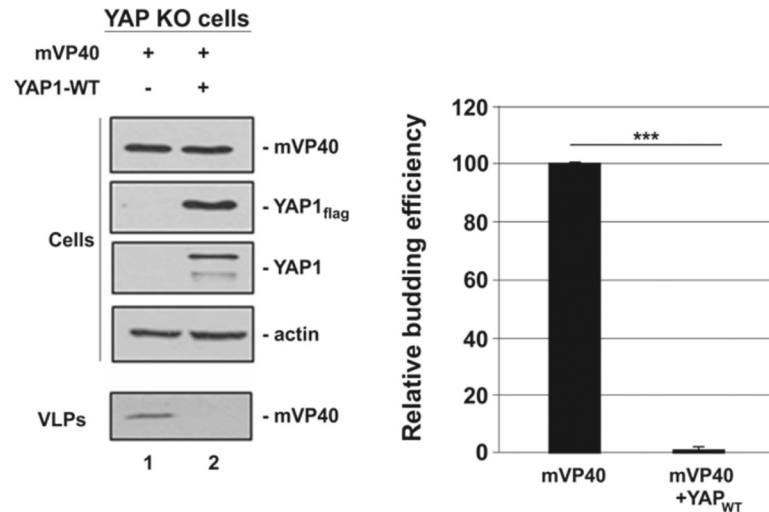
Fig 6. mVP40 VLP budding assay in YAP knockout cells. YAP knockout (KO) cells were transfected with the indicated combinations of plasmids (0.25μg/each), and both cell extracts and VLPs were harvested at 24 hrs post-transfectio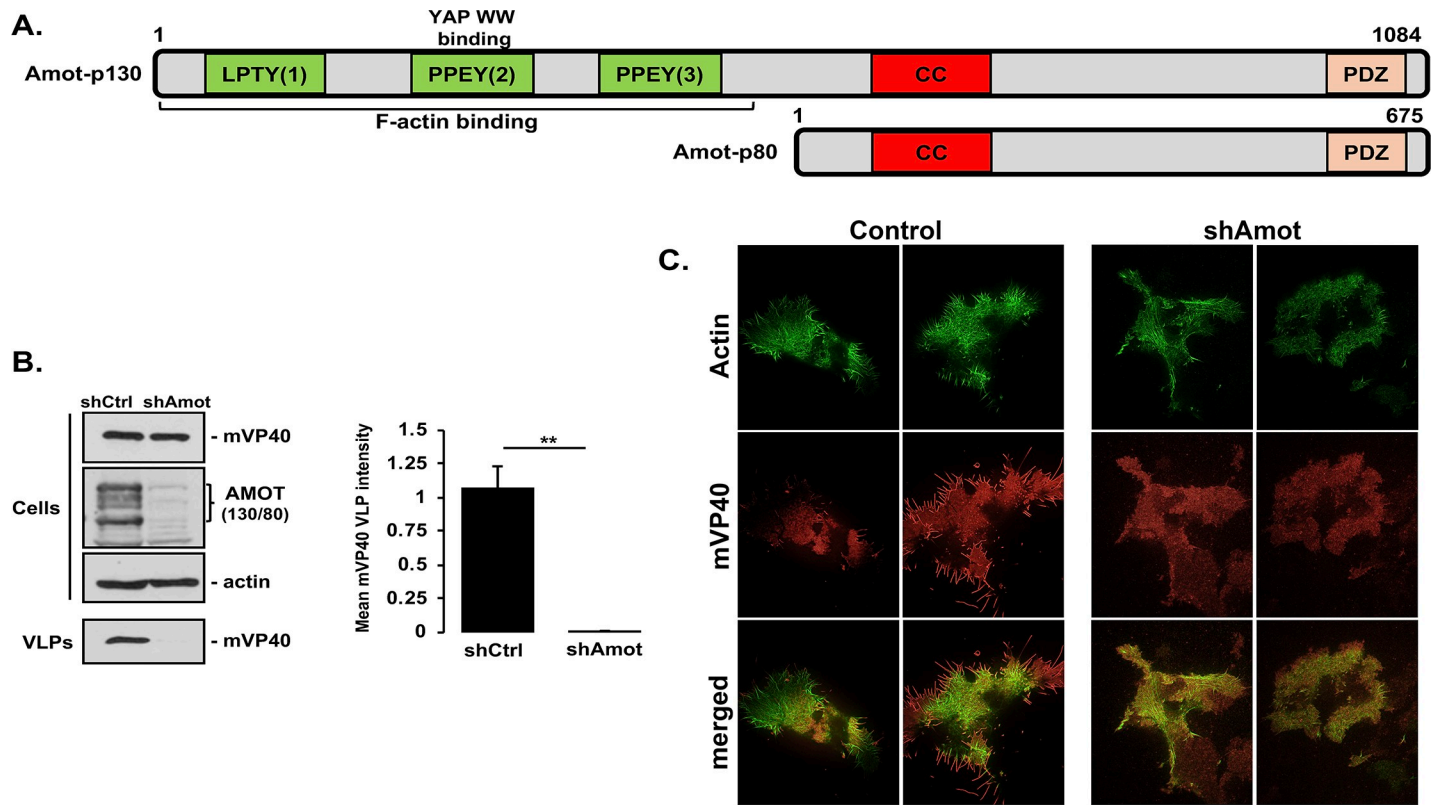n. The indicated proteins were detected and quantified in cells and VLPs by Western blotting and NIH Image-J, respectively. Bar graph represents data from at least three independent experiments. *** p<0.001.

https://doi.org/10.1371/journal.ppat.1008231.g006

transfected with mVP40 (Fig 7B), and both cell extracts and VLPs were harvested and analyzed by Western blotting. Indeed, we observed robust inhibition of mVP40 VLP egress in the shAmot cells compared to egress of mVP40 VLPs in shCtrl cells (Fig 7B). Since budding of mVP40 VLPs was reduced significantly in shAmot cells, we sought to determine whether the mechanism of inhibition correlated with Amot's role as an F-actin binding protein. Toward this end, we co-transfected either shCtrl or shAmot cells with plasmids fluorescently labeling F-actin (pCMV-LifeAct-RFP) and YFP-mVP40, and used TIRF microscopy to visualize both F-actin and mVP40 localization at the plasma membrane (Fig 7C). We observed robust localization of both F-actin and mVP40 in well-formed, prominent surface membrane projections in shCtrl cells. Interestingly, F-actin was most prominent at the bases of the membrane projections, whereas mVP40 was observed throughout the projections (Fig 7C). In contrast, shAmot cells displayed significantly fewer membrane projections than shCtrl cells, and the localization patterns of both F-actin and mVP40 appeared more diffuse and disorganized (Fig 7C). Together, these results not only suggest that expression of endogenous Amot is important for mVP40 VLP formation/protrusion at the plasma membrane and subsequent egress, but also that the mechanism by which Amot regulates VLP formation and egress may be linked to its role in binding and organizing F-actin filaments at the cell surface.

Release and spread of authentic MARV is inhibited in shAmot knockdown cells

Next, we asked whether budding and spread of authentic MARV strain Musoke would also be inhibited in the shAmot cells compared to that in shCtrl cells. Briefly, shCtrl or shAmot cells in 96-well plates were infected with MARV strain Musoke (Fig 8) [78] at MOIs of 0.01 or 0.05, and the cells were fixed at 24, 48, and 72 hours post-infection to assess virus spreading. Indeed, spread of MARV throughout the cultures was inhibited significantly in the shAmot cells compared to that observed in the shCtrl cells (Fig 8A and 8C). Similarly, release of infectious MARV was also inhibited significantly in the shAmot cells compared to that observed in the shCtrl cells (Fig 8B and 8D). Taken together, we observed that expression of endogenous

A.

B.

C.

Fig 7. VP40 VLP budding assay in AMOT control (shCtrl) or AMOT knockdown (shAmot) cells. A) Schematic diagrams of full-length angiomotin (Amot-p130) and N-terminally truncated angiomotin (Amot-p80) with key domains highlighted. Numbers represent amino acids. LPTY(1), PPEY(2), and PPEY(3) = three PPxY motifs; CC = coiled coil domain; PDZ = PSD-95/Dlg1/ZO-1 domain. **B)** AMOT expressing (shCtrl) or knockdown (shAmot) cells were transfected with mVP40 (0.25μg) and the indicated proteins were quantified in cells and VLPs by Western blotting and NIH Image-J, respectively. The bar graph represents data from at least three independent experiments. ** $p < 0.01$. **C)** shCtrl or shAmot cells were transfected with 0.5μg each of pCMV-LifeAct-RFP and YFP-mVP40 plasmids, and cells were imaged by TIRF microscopy at 24 hours post-transfection. Two representative images of F-actin alone (green), YFP-mVP40 alone (red), and merged images for both shCtrl and shAmot cells are shown. Scale bar = 10 μm.

Amot was crucial not only for VP40 VLP egress, but also for spread and egress of infectious filoviruses.

Expression of Amot overcomes YAP1-mediated inhibition of mVP40 VLP budding

Since the PPxY motifs of Amot interact strongly with the WW-domain of YAP1, we wanted to determine whether Amot-p130 could compete in a PPxY-dependent manner with mVP40 for binding to YAP1 and thus relieve the inhibitory effect of YAP1 on mVP40 VLP egress. Toward this end, HEK293T cells were transfected with the indicated combinations of plasmids (Fig 9A), and both cell extracts and VLPs were harvested and analyzed by Western blotting. As before, expression of YAP1 WT significantly inhibited egress of mVP40 VLPs (Fig 9A, compare lanes 1 + 2); however, upon co-expression of increasing amounts of Amot-p130, budding of mVP40 VLPs was rescued to near WT levels (Fig 9A, lanes 3–5). Importantly, mVP40 VLP budding was not rescued in the presence of Amot-p80, which lacks the PPxY motifs (Fig 9A, lane 6). These results were identical to those observed with TAZ-WT plus either Amot-p130 or Amot-p80 (Fig 9B). Together, these results show that ectopic expression of Amot-p130 was able to rescue budding of mVP40 VLPs in the presence of either YAP1 WT or TAZ-WT in a
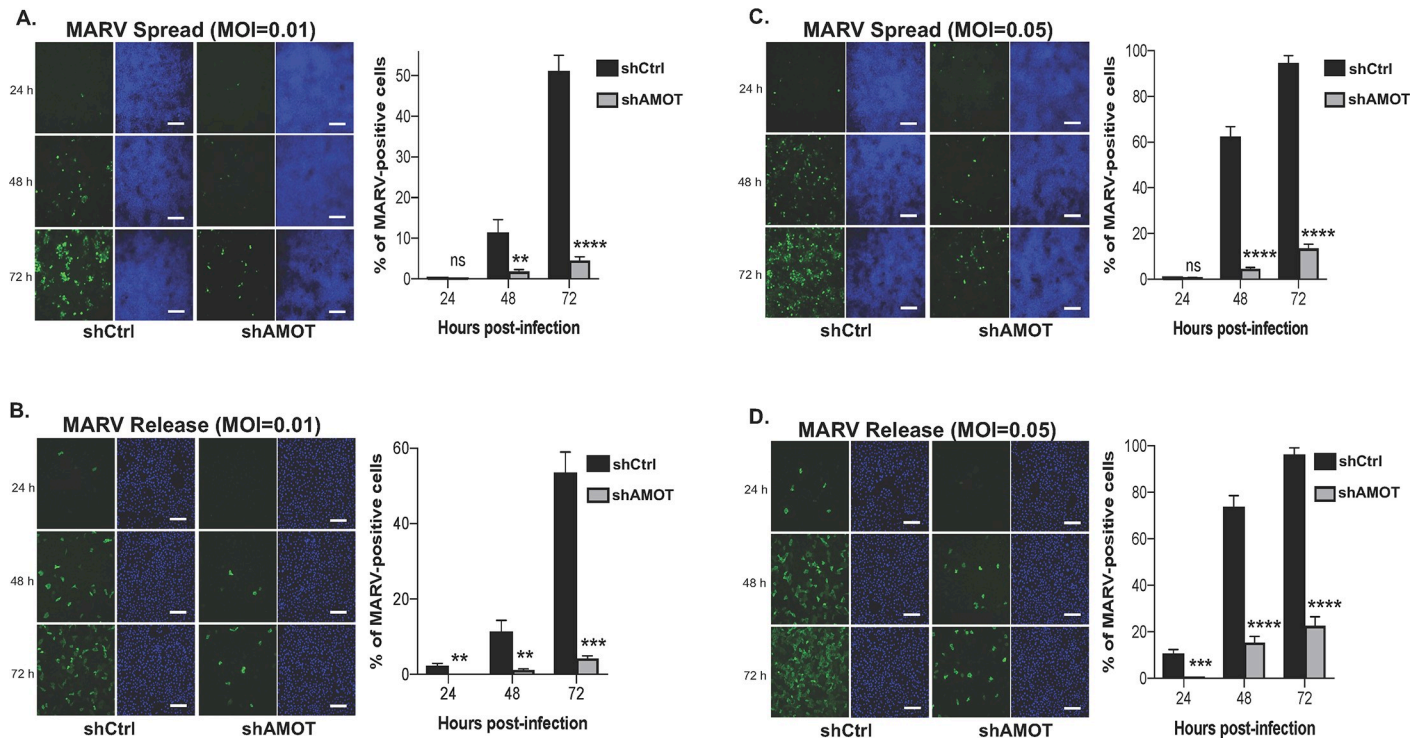
Fig 8. Spread and release of live MARV from shCtrl or shAmot cells. shCtrl or shAmot cells were infected with MARV at an MOI of either 0.01 (**A** and **B**), or 0.05 (**C** and **D**), and both virus spread (**A** and **C**) and release (**B** and **D**) were quantified at 24, 48, and 72 hours post-infection. MARV = green, Hoechst 33342-stained nuclei = blue. Bar graphs represent data from three independent experiments. Scale bars = 200 μm.

https://doi.org/10.1371/journal.ppat.1008231.g008

PPxY-dependent manner, and suggest that the competitive interplay among Amot, YAP1, TAZ, and mVP40 may be mechanistically important for either positive or negative regulation of mVP40-mediated egress.

Amot-p130 PPxY motifs 2 and 3 are important for rescue of mVP40 VLP budding

To more precisely determine whether the PPxY motifs of Amot-p130 were necessary for rescue of mVP40 VLP budding in the presence of YAP1, we used a double PPxY mutant of Amot-p130 in which PPxY motifs 2 and 3 have been mutated [68]. We chose this mutant since PPxY motifs 2 and 3 of Amot-p130 are more conventional and match more closely to the PPxY core motif conserved in mVP40 (Fig 7A). Briefly, HEK293T cells were transfected with the indicated combinations of plasmids (Fig 10), and both cell extracts and VLPs were harvested and analyzed by Western blotting. As we observed previously, YAP1 WT inhibited mVP40 VLP egress (Fig 10, lane 2), whereas the addition of an equal amount of Amot-p130 overcame this inhibition to rescue budding of mVP40 VLPs (Fig 10, lane 3). Interestingly, expression of mutant Amot-PY2/3 did not rescue budding of mVP40 VLPs, suggesting that either one or both of these PPxY motifs of Amot-p130 are critical for VLP rescue, again likely due to competition for binding to WW1 domain of YAP1.

Filoviral and host PPxY motifs can bind to WW1 domain of YAP

To complement the biochemical experiments described above, we sought to use a structure-based docking approach to assess the binding potential of the filoviral VP40 and Amot PPxY
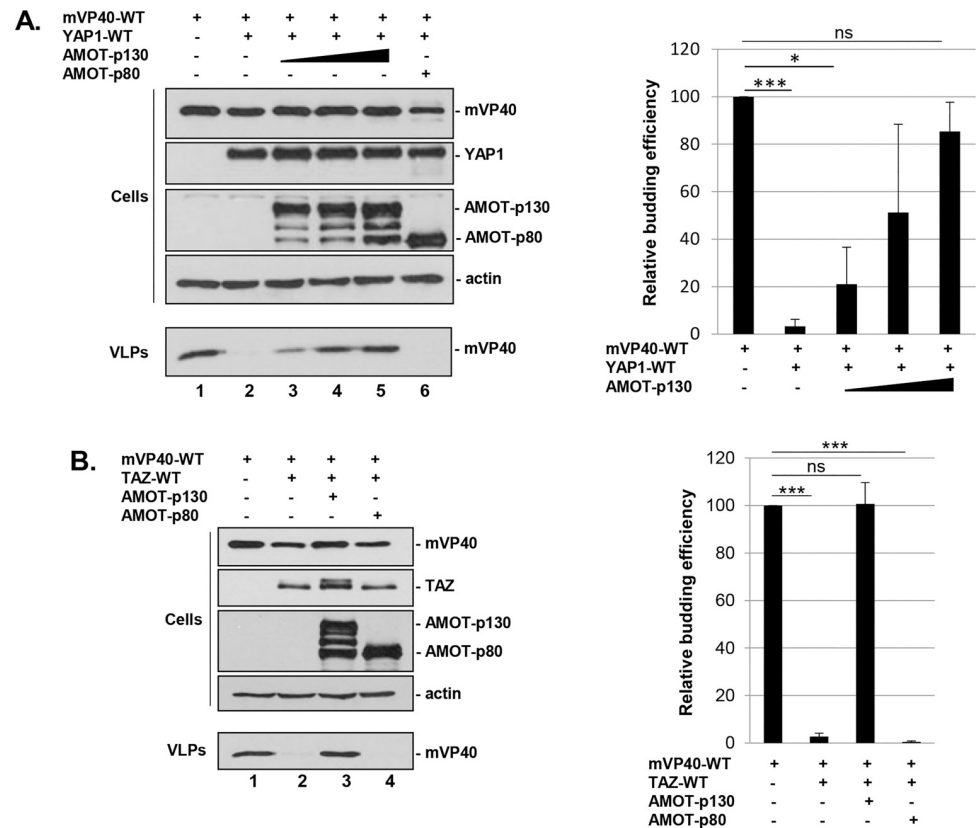
Fig 9. Angiomotin rescues budding of mVP40 VLPs in the presence of YAP or TAZ. A + B) HEK293T cells were transfected with the indicated combinations of plasmids (0.25μg of mVP40, 0.25μg/each of YAP1-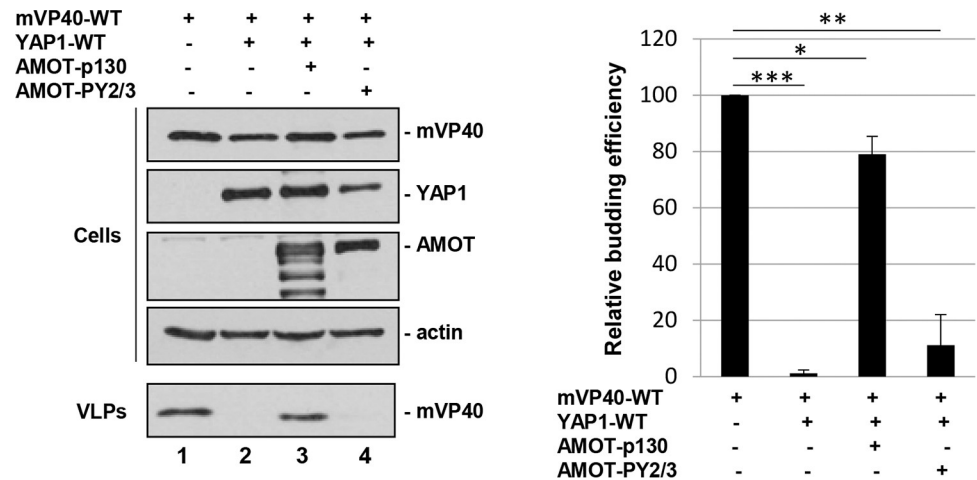WT and TAZ-WT, 0.25μg, 0.5μg or 1.0μg of Amot-p130, and 1.0μg of Amot-p80) and both cell extracts and VLPs were harvested at 24 hrs post-transfection. The indicated proteins were detected and quantified in cells and VLPs by Western blotting and NIH Image-J, respectively. Bar graphs represent data from at least three independent experiments. **A)** * $p < 0.05$, *** $p < 0.001$, ns = not significant; **B)** *** $p < 0.001$, ns = not significant.

containing peptides to interact with YAP WW1 domain (Fig 11). The YAP WW domains exhibit a typical triple-stranded anti-parallel β-sheet structure, with the glycine linker forming an unstructured loop that holds the binding peptide in close proximity to the domain. PPxY peptides exhibit a polyproline type II (PPII) helical conformation. There are two pockets that recognize the PPxY peptide; the P1 pocket is formed by the side chains of W199 and T197 and accommodates P1, and the Y pocket is a hydrophobic groove composed of sidechains from L190, H192, Q195, and T197 that fit the Y sidechain of the PPxY peptide (Fig 11).

To validate our Glide peptide docking module, we first docked the Smad7 peptide to the YAP WW1 domain. Our ability to reproduce the crystal structure of the smad7 peptide (RMSD 1.2 Å) (Fig 11A) confirmed its reliability. Next, we tested both eVP40 and mVP40 PPxY peptides as well as the three Amot-p130 PPxY peptides for their ability to dock with the PPxY binding region of YAP WW1 domain (Fig 11, panels B-F). We found that all five peptides could bind to the PPxY binding pocket of YAP WW1 domain; however, the mVP40 PPxY peptide yielded the best docking score (Emodel score of -166.8). Indeed, the tyrosine (Y) residue found before the PPxY motif in the mVP40 and the histidine (H) residue following the PPxY motif in the mVP40 peptide mediated direct interactions with the YAP WW1 domain and contributed to the strength of binding. Following the mVP40 PPxY peptide, the next strongest interactions were mediated by Amot-2, Amot-1, eVP40, and Amot-3 peptides. These

Fig 10. Angiomotin rescue of mVP40 VLP budding is dependent on Amot's PPxY motifs. HEK293T cells were transfected with the indicated combinations of plasmids (0.25μg of mVP40, 0.25μg of YAP1-WT, 1.0μg of Amot-p130, and 1.0μg of Amot-PY2/3), and both cell extracts and VLPs were harvested at 24 hrs post-transfection. Amot-PY2/3 contains mutations in PPEY motifs #2 and #3 (see Fig 6A). The indicated proteins were detected and quantified in cells and VLPs by Western blotting and NIH Image-J, respectively. Bar graph represents data from at least three independent experiments. * $p<0.05$, ** $p<0.01$, *** $p<0.001$.

https://doi.org/10.1371/journal.ppat.1008231.g010

observations support the potential for competition between filoviral and host PPxY motifs for binding to YAP WW1 domain, which not only may regulate viral egress and transmission, but also may affect the localization of YAP1 and thus its function as the major effector of the Hippo pathway.

Discussion

The PPxY L-domain motifs of EBOV and MARV VP40 interact with specific host proteins that contain one or more modular WW-domains to regulate VLP/virus assembly, egress, and spread [9,10,17,79]. As the PPxY core motif is physically and functionally conserved in a wide array of matrix proteins encoded by viruses belonging to the *Filoviridae*, *Arenaviridae*, *Retroviridae*, *Rhabdoviridae*, *and Paramyxoviridae* families [16,80], a better understanding of the breadth and function of PPxY-dependent host interactions during the budding process will likely have wide-ranging implications for the biology and pathogenesis of a plethora of viral pathogens.

Here we identified two novel mVP40 PPxY interactors, YAP1 and TAZ, that in addition to the recently identified host interactor BAG3 [81,82], are members of a growing list of WW-domain bearing host proteins that negatively regulate VP40-mediated egress. Expression of either WT YAP1 or WT TAZ led to a significant decrease in mVP40 VLP egress. Moreover, budding of mVP40 VLPs was efficient in YAP KO cells; however, upon expression of exogenous YAP1, VLP budding decreased significantly. While the identity and number of negative regulators of budding continues to expand, the majority of previously characterized host PPxY interactors positively affect egress (*e.g.* members of the HECT family of E3 ubiquitin ligases). We speculate that viruses such as EBOV and MARV have evolved mechanisms to mimic the modular nature of host interactions to hijack or recruit specific host proteins to facilitate or enhance virus egress and spread. Conversely, we envision host cells countering with innate defense mechanisms that target these conserved viral motifs to inhibit or disrupt virion assembly and egress. For example, BAG3 is a co-chaperone and cell survival protein recently shown to interact with the mVP40 and eVP40 PPxY motifs to sequester VP40 in the cytoplasm, away
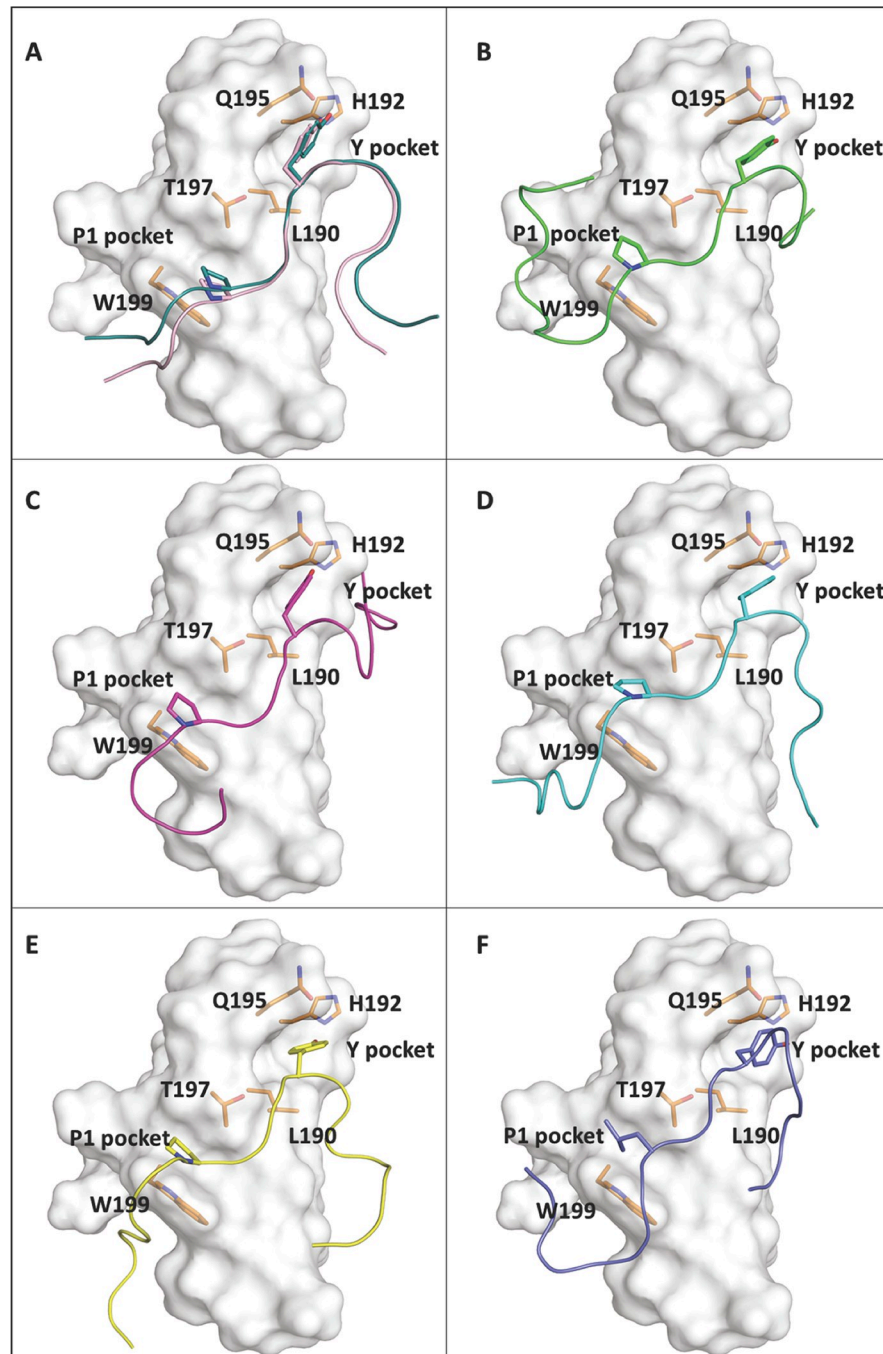
Fig 11. Protein-peptide docking poses. The protein-peptide docking poses are shown for: **A)** the NMR structure of YAP WW1-smad7 peptide (GESP**PPPY**SRYPMD) complex (light pink color) and the docking pose of smad7 peptide (control, deep teal color), **B)** YAP WW1 domain-eVP40 peptide (MRRVILPTA**PPEY**MEAI) (green), **C)** YAP WW1 domain-mVP40 peptide (MQYLN**PPPY**ADHGANQL) (magenta), **D)** YAP WW1 domain-Amot peptide 1 (GMEHRGP**PPEY**PFKGMP) (cyan), **E)** YAP WW1 domain-Amot peptide 2 (QLMRYQH**PPEY**GAARPA) (yellow), and **F)** YAP WW1 domain-Amot peptide 3 (MQNNEE**LPTY**EEAKVQ) (purple). The first Proline (P1) of the PPxY motif (or L of LPTY in Amot peptide 3) occupies the P1 pocket of YAP WW1 domain which is formed by T197 and W199, and the Y sidechain of the PPxY motif occupies the Y pocket (hydrophobic groove composed by L190, H192, Q195, and T197) of YAP WW1 domain.

https://doi.org/10.1371/journal.ppat.1008231.g011

from the site of budding at the plasma membrane [81,82]. Interestingly, the BAG3 WW-domain has been reported to engage in the PPxY/WW-domain interactions that regulate YAP/TAZ signaling, and as a result, BAG3 may modulate YAP/TAZ-mediated co-transcriptional activity of genes involved in cell proliferation, actin dynamics and crosslinking, and cell adhesion/migration [83].

As the downstream effector of the Hippo pathway, YAP can either be sequestered in the cytoplasm in a phosphorylated form (Hippo ON), or shuttled into the nucleus in an unphosphorylated form (Hippo OFF), where it will engage TEAD transcription factors to upregulate genes involved in cell proliferation. We found that ectopic expression of a phosphorylation mutant of YAP1 (localized predominantly in the nucleus) partially rescued egress of mVP40 VLPs (Fig 4), likely due in part to the inability of nuclear YAP1 to physically engage mVP40 and sequester it away from the plasma membrane. In addition, treatment of mVP40-expressing cells with EGF to trigger translocation of endogenous YAP1 into the nucleus, resulted in a dose-dependent increase in VLP budding (Fig 5). It is also tempting to speculate that once YAP1 enters the nucleus, upregulation of genes involved in cell proliferation/migration, actin polymerization, and filopodia formation may also promote an intracellular environment that is favorable for efficient VLP formation and/or egress. These studies, as well as those using authentic filoviruses, will be necessary to demonstrate a role for the endogenous Hippo pathway in impacting filovirus replication.

One of the key regulators of YAP1 localization and activity is Amot, which binds strongly to the first WW-domain of YAP1 *via* one of its multiple N-terminal PPxY motifs [84]. Amot, along with other family members, plays an important role in the biology of the vascular system, and Amot has been linked previously to budding of other RNA viruses [85–88]. Interestingly, we observed a dose-dependent rescue of mVP40 VLP budding when increasing amounts of Amot were added to cells co-expressing mVP40 and either YAP1 or TAZ. Moreover, we used shCtrl (expressing endogenous Amot) and an shAmot knockdown cell line to show that endogenous Amot was critical for efficient egress of mVP40 VLPs (Fig 7B). Images from TIRF microcopy provided mechanistic insights into the observed Amot-mediated changes in VLP egress by revealing significantly distinct patterns of localization of both F-actin filaments and mVP40 expressed at the plasma membrane of either shCtrl or shAmot cells (Fig 7C). Indeed, these findings revealed that the formation and organization of F-actin filaments sharply aligned with mVP40 at the bases of the visible VLP membrane projections in shCtrl cells, whereas this alignment and organization of F-actin with mVP40 VLPs was largely absent in shAmot cells (Fig 7C). Importantly, we found that egress and spread of live MARV (Fig 7) was also significantly more robust in shCtrl cells expressing endogenous Amot than that observed in shAmot knockdown cells at 24, 48, and 72 hours post-infection. The ability of Amot to rescue budding of mVP40 VLPs in the presence of YAP1 was likely due to competition between the PPxY motifs of Amot and those of mVP40 for binding to endogenous YAP1. Indeed, Amot-p80, which lacks all of the N-terminal PPxY motifs, was unable to rescue mVP40 VLP budding, and we demonstrated that PPxY motifs 2 and 3 of Amot-p130 were critical for rescue of mVP40 VLP egress. Additionally, the well-documented physical interaction of Amot with LATS1/2 kinases, which results in the activation of the kinases and sequestration of phosphorylated YAP1 and TAZ proteins in the cytoplasm, deserves careful study in the context of VP40 signalling [76].

Amot binds and sequesters YAP1 on both actin filaments and at cellular tight junctions (Fig 12) [59,60,62,64,65,89–94]. The Amot/YAP1 complex may also enter the nucleus leading to upregulation of a set of genes that may be distinct from those upregulated by YAP1 alone [61,64,66]. Thus, it is possible that modular competition between PPxY motifs of filoviral VP40 and Amot for binding to the WW domain of YAP1 could impact several processes in
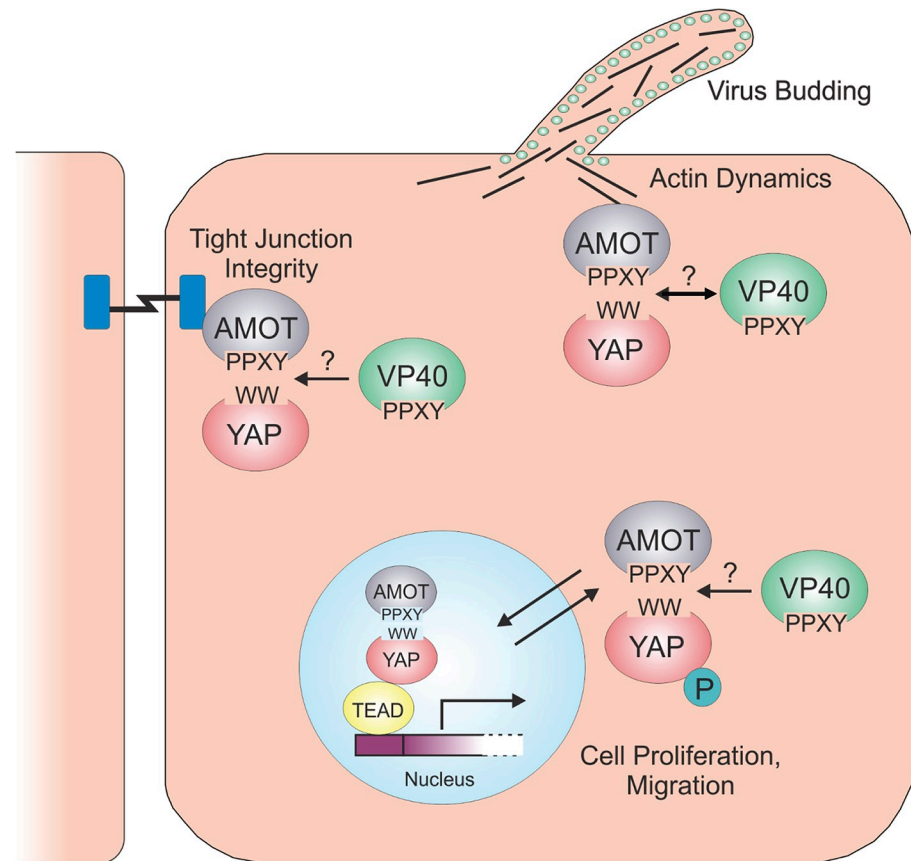
Fig 12. Working model of modular competition between filovirus VP40 and Hippo pathway components YAP and AMOT. Potential competition (?) between the PPxY motifs of filovirus VP40 and those of AMOT for binding to WW-domains of YAP (and/or TAZ) may affect cellular processes including, actin dynamics and filopodia formation, tight junction formation and integrity, and upregulation of genes involved in cell proliferation and migration.

the host cell including: 1) actin dynamics and polymerization, 2) tight junction formation and integrity, and 3) upregulation of cell proliferation genes (Fig 12). Our data indicate that competition for binding among YAP1/Amot/mVP40 complexes, as well as Amot's role in regulating F-actin dynamics at the plasma membrane [62,90], may both play a mechanistic role in impacting VP40-mediated egress.

Lastly, filovirus infection could potentially influence Hippo signaling. For example, if VP40 competes with Amot for binding and/or sequestering YAP1 in the cytoplasm, this may affect YAP1-regulated genes and impact filovirus egress and spread. Indeed, several YAP1-responsive genes encode proteins involved in actin polymerization, filopodia formation, and plasma membrane projections involved in cell migration. Such outcomes would be beneficial for maximal levels of filovirus budding at the plasma membrane. Studies are now underway to identify and quantify both up- and down-regulated genes in cells expressing various combination of YAP1/Amot/VP40 to determine whether nuclear localized and transcriptionally active YAP1 regulates VP40-mediated egress. These findings may provide new insights into how potentially altering Hippo signaling pharmaceutically could perhaps impact virus budding, spread, and pathogenesis.

In sum, we identified YAP1 and TAZ as two novel WW-domain interactors with the PPxY motif of mVP40, that like BAG3, inhibited mVP40-mediated egress in a PPxY/WW-domain

dependent manner. These findings are the first to link key effectors of the Hippo pathway to the biology and perhaps pathogenesis of filoviruses. These findings provide important insights into the roles of novel host proteins and a new cellular pathway in regulating filovirus VP40-mediated egress. The interplay among VP40/YAP1/TAZ/Amot may have wide ranging biological and pathological implications in filovirus infection and disease, and thus a more comprehensive understanding of these virus-host interactions may be helpful in the development of future antiviral therapies. Moreover, since many additional RNA viruses also contain PPxY L-domain motifs, these findings may implicate the Hippo pathway in the biology and egress of a wide array of viral pathogens.

Materials and methods

Cell lines and antisera

HEK293T, HEK293A YAP knockout cells (kindly provided by K-L. Guan, University of California, San Diego), HEK293T-based shCtrl, and shAmot cells (kindly provided by J. Kissil, Scripps Research Institute, FL) were maintained in Dulbecco's modified Eagle's medium (DMEM) supplemented with 10% fetal calf serum (FCS), penicillin (100 U/ml)/streptomycin (100μg/ml) at 37˚C in a humidified 5% CO_2 incubator [64,75]. Antisera used include: anti-FLAG antibody (Fitzgerald, CAT# 10R-7750) to detect ectopically expressed Flag-tagged mVP40 and Flag-tagged YAP1; anti-YAP1 antibody (clone 1A12, Cell signaling, CAT# 12395S); anti-ß-actin (Gene Tex, CAT# GT5512); anti-GST (Sigma); anti-Amot (EMD Millipore); anti-HA to detect HA-tagged TAZ (Sigma); anti-rabbit IgG-HRP (GE Healthcare, CAT# NA934V); or anti-mouse IgG-HRP (GE Healthcare, CAT# NA931V).

Expression and Purification of GST-YAP1 WW fusion proteins

Expression and purification of GST fusion proteins from pGEX-YAP-WW1 and pGEX-YAP-WW2 plasmids (kindly provided by M. Bedford, Univ. of Texas) were performed as described previously [95]. Briefly, pGEX-YAP-WW1 and pGEX-YAP-WW2 plasmids were transformed into *E. coli* BL21(DE3) cells and single colonies were cultured in 10ml of LB media overnight with shaking at 37˚C. The overnight culture was added into 100ml of fresh LB broth and grown at 37˚C for one hour with shaking. GST-WW domain fusion proteins were induced with isopropyl-β-d-thiogalactopyranoside (IPTG) (0.1 mM) for 4 h at 30˚C. Bacterial cultures were centrifuged at 5,000 rpm for 10 min at 4˚C, and lysates were extracted by using B-PER bacterial protein extract reagent according to the protocol supplied by the manufacturer (Pierce). GST-YAP-WW1, GST-YAP-WW2, and GST-TAZ-WW domain fusion proteins were purified with glutathione-Sepharose 4B and eluted with elution buffer (100 mM Tris-Cl [pH 8.0], 120 mM NaCl, 30 mM reduced glutathione). Purified proteins were analyzed on SDS-PAGE gels and stained with Coomassie blue.

GST-WW/mVP40 pulldown assay

GST-YAP-WW1, GST-YAP-WW2, and GST-TAZ-WW domain fusion proteins (10μg) were incubated with glutathione-Sepharose 4B beads in 500 μl of nonionic detergent-based solution in B-PER bacterial protein extract reagent kit overnight at 4˚C. The glutathione-Sepharose 4B beads were washed 3 times with 1x PBS and then incubated with cell extracts from mock or mVP40 transfected HEK293T cells overnight at 4˚C. The beads were then washed 5x with 1x mild buffer and suspended in 30μl of 2x loading buffer with boiling. Flag-tagged mVP40 protein was detected by SDS-PAGE and Western blotting with anti-flag antibody.

Confocal microscopy

HEK293T cells on glass slides were transfected with YFP-mVP40, CFP-YAP1-WT, and/or CFP-YAP1 WW mutant plasmids for 20 hours. Cells were fixed with 4% paraformaldehyde (Affymetrix) and permeabilized with 0.1% TritonX-100, and then mounted with Prolong gold anti-fade mountant with DAPI (Thermofisher scientific-p36935). Images were obtained on a Leica SP5 inverted confocal microscope with a 100x (NA 1.46) objective lens. The confocal images were subsequently deconvolved with Huygens Essential deconvolution software. CFP-YAP1-WT and CFP-YAP1 WW mutant plasmids were kindly provided by K-L Guan.

TIRF microscopy

HEK293T control (shCtrl) and Amot knockdown (shAmot) cells were plated onto coverglass bottom 35mm dishes (MatTek) and 24h later were co-transfected with plasmids expressing pCMV-LifeAct-RFP (ibidi) and YFP-mVP40. Just prior to imaging, the cells were stained with Deep Red CellMask plasma membrane stain (Invitrogen). Dishes were placed onto the stage of a GE DeltaVision OMX SR microscope and maintained at 37˚C and 5% CO_2 in a stage-top incubator. Approximately 20 cells per group were randomly chosen and imaged in SIM-TIRF mode. SIM super-resolution images were reconstructed from the acquired TIRF images.

VP40 VLP budding assay

HEK293T, YAP KO, shCtrl, or shAmot cells in collagen-coated six-well plates were transfected with the indicated plasmids (total plasmid DNA was equivalent in all samples) using Lipofecta-mine reagent (Invitrogen) and the protocol of the supplier. At 6 hours post-transfection, OPTI-MEM was added for 24 hours. Culture media was centrifuged at 351 x g for 10 minutes to remove cellular debris, layered onto a 20% sucrose cushion in STE buffer and centrifuged at 220,000 x g for 2 hours at 4˚C. The VP40 VLP pellet was suspended in STE buffer at 4˚C over-night. The indicated proteins were analyzed by SDS-PAGE and Western-blotting, and proteins were quantified using NIH Image-J software.

Protein-peptide docking

Protein-peptide docking analysis was performed using Glide module in Schrödinger. The pro-tein structure of YAP WW1 domain (PDB ID: 2LTW) was downloaded from PDB [96] and was prepared with the Protein Preparation Wizard tool in Schrodinger. The peptides were built using Maestro and generated multiple conformers using the MacroModel sampling method. The receptor grid for peptide docking purposes was prepared with default settings using the peptide ligand to define the grid center. The peptide conformers were docked using Glide SP-PEP protocol [97].

Filovirus stocks

All experiments with replication competent MARV were performed in the biosafety level 4 (BSL-4) laboratory at the Texas Biomedical Research Institute (San Antonio, TX). MARV strain Musoke (NCBI accession number NC_001608) was obtained from the virus repository at the Texas Biomedical Research Institute, San Antonio, TX [78].

Filovirus spread

shCtrl and shAmot cells were grown in 96-well plates and incubated with MARV at MOI of 0.01 or 0.05. Three separate plates were challenged in triplicate for each MOI. After 1 h, inocu-lum was removed, cells washed with medium, and new medium was added to wells. Cells were

fixed 24h, 48h, or 72h after virus challenge and then stained with Hoechst 33342. MARV-infected cells were also stained with anti-VLP antibody. Cells were photographed using a Nikon Ti-Eclipse microscope running high content analysis software (Nikon, Tokyo, Japan). The numbers of cell nuclei and infected cells were counted using Cell Profiler software (Broad Institute, Boston, MA).

Filovirus release

To assess release of replication-competent MARV from shCtrl or shAmot cells, the supernatants of infected cells were harvested and overlaid onto monolayers of Vero cells (American Type Culture Collection; ATCC, Manassas, VA) grown in 96-well plates. After 24 h, cells were fixed, stained, and analyzed as above.

Statistical analysis

Absolute intensities for each immunoblot lane were normalized to the intensity of the first lane of the blot and averaged across at least three replicates (collected from 3 or more separate transfections). Mean normalized intensity ±SD is shown. Due to observed inequality of variance between the groups (determined by F-test p-value <0.05), Welch's t-test was used to determine statistical significance. For live virus data, mean percentage ±SD is shown from 3 independent experiments. Viral spreading was compared using the student's t-test. All p values were designated using the following symbolic representation: ns = $p > 0.05$, * = $p \leq 0.5$, ** = $p \leq 0.01$, *** = $p \leq 0.001$, **** = $p \leq 0.0001$.

Supporting information

S1 Table. Host WW-Domains Interacting with the mVP40 PPxY Peptide. WW-domains from the listed host proteins were shown to interact with the PPxY motif present within mVP40.
(PDF)

Acknowledgments

Author Contributions

Conceptualization: Ronald N. Harty.

Data curation: Ziying Han, Shantoshini Dash, Cari A. Sagum, Gordon Ruthel, Chaitanya K. Jaladanki, Corbett T. Berry, Michael P. Schwoerer, Nina M. Harty, Olena Shtanko.

Formal analysis: Corbett T. Berry.

Funding acquisition: Marius Sudol, Ronald N. Harty.

Investigation: Ziying Han, Shantoshini Dash, Cari A. Sagum, Gordon Ruthel, Chaitanya K. Jaladanki, Hao Fan, Olena Shtanko.

Methodology: Ziying Han, Cari A. Sagum, Gordon Ruthel, Chaitanya K. Jaladanki, Michael P. Schwoerer, Mark T. Bedford, Hao Fan, Sachdev S. Sidhu, Marius Sudol, Olena Shtanko.

Project administration: Ronald N. Harty.

Resources: Bruce D. Freedman, Mark T. Bedford, Marius Sudol, Olena Shtanko, Ronald N. Harty.

Supervision: Bruce D. Freedman, Mark T. Bedford, Hao Fan, Ronald N. Harty.

Writing – original draft: Ziying Han, Marius Sudol, Olena Shtanko, Ronald N. Harty.

Writing – review & editing: Ronald N. Harty.

References

1. Coffin KM, Liu J, Warren TK, Blancett CD, Kuehl KA, et al. (2018) Persistent Marburg Virus Infection in the Testes of Nonhuman Primate Survivors. Cell host & microbe 24: 405–416 e403.

2. Schindell BG, Webb AL, Kindrachuk J (2018) Persistence and Sexual Transmission of Filoviruses. Viruses 10.

3. Yeh S, Varkey JB, Crozier I (2015) Persistent Ebola Virus in the Eye. The New England journal of medicine 373: 1982–1983.

4. Zeng X, Blancett CD, Koistinen KA, Schellhase CW, Bearss JJ, et al. (2017) Identification and pathological characterization of persistent asymptomatic Ebola virus infection in rhesus monkeys. Nat Microbiol 2: 17113. https://doi.org/10.1038/nmicrobiol.2017.113 PMID: 28715405

5. Han Z, Madara JJ, Liu Y, Liu W, Ruthel G, et al. (2015) ALIX Rescues Budding of a Double PTAP/PPEY L-Domain Deletion Mutant of Ebola VP40: A Role for ALIX in Ebola Virus Egress. The Journal of infectious diseases 212 Suppl 2: S138–145.

6. Lu J, Qu Y, Liu Y, Jambusaria R, Han Z, et al. (2013) Host IQGAP1 and Ebola virus VP40 interactions facilitate virus-like particle egress. Journal of virology 87: 7777–7780. https://doi.org/10.1128/JVI.00470-13 PMID: 23637409

7. Liu Y, Lee MS, Olson MA, Harty RN (2011) Bimolecular Complementation to Visualize Filovirus VP40-Host Complexes in Live Mammalian Cells: Toward the Identification of Budding Inhibitors. Advances in virology 2011.

8. Noda T, Ebihara H, Muramoto Y, Fujii K, Takada A, et al. (2006) Assembly and budding of Ebolavirus. PLoS pathogens 2: e99. https://doi.org/10.1371/journal.ppat.0020099 PMID: 17009868

9. Hartlieb B, Weissenhorn W (2006) Filovirus assembly and budding. Virology 344: 64–70. https://doi.org/10.1016/j.virol.2005.09.018 PMID: 16364737

10. Jasenosky LD, Kawaoka Y (2004) Filovirus budding. Virus research 106: 181–188. https://doi.org/10.1016/j.virusres.2004.08.014 PMID: 15567496

11. Yasuda J, Nakao M, Kawaoka Y, Shida H (2003) Nedd4 regulates egress of Ebola virus-like particles from host cells. Journal of virology 77: 9987–9992. https://doi.org/10.1128/JVI.77.18.9987-9992.2003 PMID: 12941909

12. Timmins J, Schoehn G, Ricard-Blum S, Scianimanico S, Vernet T, et al. (2003) Ebola virus matrix protein VP40 interaction with human cellular factors Tsg101 and Nedd4. Journal of molecular biology 326: 493–502. https://doi.org/10.1016/s0022-2836(02)01406-7 PMID: 12559917

13. Harty RN, Brown ME, Wang G, Huibregtse J, Hayes FP (2000) A PPxY motif within the VP40 protein of Ebola virus interacts physically and functionally with a ubiquitin ligase: implications for filovirus budding. Proceedings of the National Academy of Sciences of the United States of America 97: 13871–13876. https://doi.org/10.1073/pnas.250277297 PMID: 11095724

14. Bieniasz PD (2006) Late budding domains and host proteins in enveloped virus release. Virology 344: 55–63. https://doi.org/10.1016/j.virol.2005.09.044 PMID: 16364736

15. Calistri A, Salata C, Parolin C, Palu G (2009) Role of multivesicular bodies and their components in the egress of enveloped RNA viruses. Reviews in medical virology 19: 31–45. https://doi.org/10.1002/rmv.588 PMID: 18618839

16. Chen BJ, Lamb RA (2008) Mechanisms for enveloped virus budding: can some viruses do without an ESCRT? Virology 372: 221–232. https://doi.org/10.1016/j.virol.2007.11.008 PMID: 18063004

17. Harty RN (2009) No exit: targeting the budding process to inhibit filovirus replication. Antiviral research 81: 189–197. https://doi.org/10.1016/j.antiviral.2008.12.003 PMID: 19114059

18. Irie T, Licata JM, Harty RN (2005) Functional characterization of Ebola virus L-domains using VSV recombinants. Virology 336: 291–298. https://doi.org/10.1016/j.virol.2005.03.027 PMID: 15892969

19. Liu Y, Harty RN (2010) Viral and host proteins that modulate filovirus budding. Future virology 5: 481–491. https://doi.org/10.2217/FVL.10.33 PMID: 20730024

20. Urata S, de la Torre JC (2011) Arenavirus budding. Advances in virology 2011: 180326. https://doi.org/10.1155/2011/180326 PMID: 22312335

21. Han Z, Lu J, Liu Y, Davis B, Lee MS, et al. (2014) Small-molecule probes targeting the viral PPxY-host Nedd4 interface block egress of a broad range of RNA viruses. Journal of virology 88: 7294–7306. https://doi.org/10.1128/JVI.00591-14 PMID: 24741084

22. Lewis B, Whitney S, Hudacik L, Galmin L, Huaman MC, et al. (2014) Nedd4-mediated increase in HIV-1 Gag and Env proteins and immunity following DNA-vaccination of BALB/c mice. PloS one 9: e91267. https://doi.org/10.1371/journal.pone.0091267 PMID: 24614057

23. Sette P, Nagashima K, Piper RC, Bouamr F (2013) Ubiquitin conjugation to Gag is essential for ESCRT-mediated HIV-1 budding. Retrovirology 10: 79. https://doi.org/10.1186/1742-4690-10-79 PMID: 23895345

24. Zhadina M, Bieniasz PD (2010) Functional interchangeability of late domains, late domain cofactors and ubiquitin in viral budding. PLoS pathogens 6: e1001153. https://doi.org/10.1371/journal.ppat.1001153 PMID: 20975941

25. Weiss ER, Popova E, Yamanaka H, Kim HC, Huibregtse JM, et al. (2010) Rescue of HIV-1 release by targeting widely divergent NEDD4-type ubiquitin ligases and isolated catalytic HECT domains to Gag. PLoS pathogens 6: e1001107. https://doi.org/10.1371/journal.ppat.1001107 PMID: 20862313

26. Sette P, Jadwin JA, Dussupt V, Bello NF, Bouamr F (2010) The ESCRT-associated protein Alix recruits the ubiquitin ligase Nedd4-1 to facilitate HIV-1 release through the LYPXnL L domain motif. Journal of virology 84: 8181–8192. https://doi.org/10.1128/JVI.00634-10 PMID: 20519395

27. Urata S, Yasuda J (2010) Regulation of Marburg virus (MARV) budding by Nedd4.1: a different WW domain of Nedd4.1 is critical for binding to MARV and Ebola virus VP40. The Journal of general virology 91: 228–234. https://doi.org/10.1099/vir.0.015495-0 PMID: 19812267

28. Usami Y, Popov S, Popova E, Inoue M, Weissenhorn W, et al. (2009) The ESCRT pathway and HIV-1 budding. Biochemical Society transactions 37: 181–184. https://doi.org/10.1042/BST0370181 PMID: 19143627

29. Calistri A, Del Vecchio C, Salata C, Celestino M, Celegato M, et al. (2009) Role of the feline immunodeficiency virus L-domain in the presence or absence of Gag processing: involvement of ubiquitin and Nedd4-2s ligase in viral egress. Journal of cellular physiology 218: 175–182. https://doi.org/10.1002/jcp.21587 PMID: 18792916

30. Pincetic A, Medina G, Carter C, Leis J (2008) Avian sarcoma virus and human immunodeficiency virus, type 1 use different subsets of ESCRT proteins to facilitate the budding process. The Journal of biological chemistry 283: 29822–29830. https://doi.org/10.1074/jbc.M804157200 PMID: 18723511

31. Chung HY, Morita E, von Schwedler U, Muller B, Krausslich HG, et al. (2008) NEDD4L overexpression rescues the release and infectivity of human immunodeficiency virus type 1 constructs lacking PTAP and YPXL late domains. Journal of virology 82: 4884–4897. https://doi.org/10.1128/JVI.02667-07 PMID: 18321968

32. Zhadina M, McClure MO, Johnson MC, Bieniasz PD (2007) Ubiquitin-dependent virus particle budding without viral protein ubiquitination. Proceedings of the National Academy of Sciences of the United States of America 104: 20031–20036. https://doi.org/10.1073/pnas.0708002104 PMID: 18056634

33. Urata S, Noda T, Kawaoka Y, Yokosawa H, Yasuda J (2006) Cellular factors required for Lassa virus budding. Journal of virology 80: 4191–4195. https://doi.org/10.1128/JVI.80.8.4191-4195.2006 PMID: 16571837

34. Klinger PP, Schubert U (2005) The ubiquitin-proteasome system in HIV replication: potential targets for antiretroviral therapy. Expert review of anti-infective therapy 3: 61–79. https://doi.org/10.1586/14787210.3.1.61 PMID: 15757458

35. Vana ML, Tang Y, Chen A, Medina G, Carter C, et al. (2004) Role of Nedd4 and ubiquitination of Rous sarcoma virus Gag in budding of virus-like particles from cells. Journal of virology 78: 13943–13953. https://doi.org/10.1128/JVI.78.24.13943-13953.2004 PMID: 15564502

36. Sakurai A, Yasuda J, Takano H, Tanaka Y, Hatakeyama M, et al. (2004) Regulation of human T-cell leukemia virus type 1 (HTLV-1) budding by ubiquitin ligase Nedd4. Microbes and infection / Institut Pasteur 6: 150–156.

37. Yasuda J, Hunter E, Nakao M, Shida H (2002) Functional involvement of a novel Nedd4-like ubiquitin ligase on retrovirus budding. EMBO reports 3: 636–640. https://doi.org/10.1093/embo-reports/kvf132 PMID: 12101095

38. Harty RN, Brown ME, McGettigan JP, Wang G, Jayakar HR, et al. (2001) Rhabdoviruses and the cellular ubiquitin-proteasome system: a budding interaction. Journal of virology 75: 10623–10629. https://doi.org/10.1128/JVI.75.22.10623-10629.2001 PMID: 11602704

39. Kikonyogo A, Bouamr F, Vana ML, Xiang Y, Aiyar A, et al. (2001) Proteins related to the Nedd4 family of ubiquitin protein ligases interact with the L domain of Rous sarcoma virus and are required for gag budding from cells. Proceedings of the National Academy of Sciences of the United States of America 98: 11199–11204. https://doi.org/10.1073/pnas.201268998 PMID: 11562473

40. Licata JM, Simpson-Holley M, Wright NT, Han Z, Paragas J, et al. (2003) Overlapping motifs (PTAP and PPEY) within the Ebola virus VP40 protein function independently as late budding domains: involvement of host proteins TSG101 and VPS-4. Journal of virology 77: 1812–1819. https://doi.org/10.1128/JVI.77.3.1812-1819.2003 PMID: 12525615

41. Bouamr F, Melillo JA, Wang MQ, Nagashima K, de Los Santos M, et al. (2003) PPPYVEPTAP motif is the late domain of human T-cell leukemia virus type 1 Gag and mediates its functional interaction with cellular proteins Nedd4 and Tsg101 [corrected]. Journal of virology 77: 11882–11895. https://doi.org/10.1128/JVI.77.22.11882-11895.2003 PMID: 14581525

42. Blot V, Perugi F, Gay B, Prevost MC, Briant L, et al. (2004) Nedd4.1-mediated ubiquitination and subsequent recruitment of Tsg101 ensure HTLV-1 Gag trafficking towards the multivesicular body pathway prior to virus budding. Journal of cell science 117: 2357–2367. https://doi.org/10.1242/jcs.01095 PMID: 15126635

43. Martin-Serrano J, Perez-Caballero D, Bieniasz PD (2004) Context-dependent effects of L domains and ubiquitination on viral budding. Journal of virology 78: 5554–5563. https://doi.org/10.1128/JVI.78.11.5554-5563.2004 PMID: 15140952

44. Medina G, Pincetic A, Ehrlich LS, Zhang Y, Tang Y, et al. (2008) Tsg101 can replace Nedd4 function in ASV Gag release but not membrane targeting. Virology 377: 30–38. https://doi.org/10.1016/j.virol.2008.04.024 PMID: 18555885

45. Usami Y, Popov S, Popova E, Gottlinger HG (2008) Efficient and specific rescue of human immunodeficiency virus type 1 budding defects by a Nedd4-like ubiquitin ligase. Journal of virology 82: 4898–4907. https://doi.org/10.1128/JVI.02675-07 PMID: 18321969

46. Einbond A, Sudol M (1996) Towards prediction of cognate complexes between the WW domain and proline-rich ligands. FEBS letters 384: 1–8. https://doi.org/10.1016/0014-5793(96)00263-3 PMID: 8797792

47. Chen HI, Einbond A, Kwak SJ, Linn H, Koepf E, et al. (1997) Characterization of the WW domain of human yes-associated protein and its polyproline-containing ligands. The Journal of biological chemistry 272: 17070–17077. https://doi.org/10.1074/jbc.272.27.17070 PMID: 9202023

48. Chen HI, Sudol M (1995) The WW domain of Yes-associated protein binds a proline-rich ligand that differs from the consensus established for Src homology 3-binding modules. Proceedings of the National Academy of Sciences of the United States of America 92: 7819–7823. https://doi.org/10.1073/pnas.92.17.7819 PMID: 7644498

49. Linn H, Ermekova KS, Rentschler S, Sparks AB, Kay BK, et al. (1997) Using molecular repertoires to identify high-affinity peptide ligands of the WW domain of human and mouse YAP. Biological chemistry 378: 531–537. https://doi.org/10.1515/bchm.1997.378.6.531 PMID: 9224934

50. Espejo A, Cote J, Bednarek A, Richard S, Bedford MT (2002) A protein-domain microarray identifies novel protein-protein interactions. The Biochemical journal 367: 697–702. https://doi.org/10.1042/BJ20020860 PMID: 12137563

51. Ardestani A, Lupse B, Maedler K (2018) Hippo Signaling: Key Emerging Pathway in Cellular and Whole-Body Metabolism. Trends Endocrinol Metab 29: 492–509. https://doi.org/10.1016/j.tem.2018.04.006 PMID: 29739703

52. Chen YA, Lu CY, Cheng TY, Pan SH, Chen HF, et al. (2019) WW Domain-Containing Proteins YAP and TAZ in the Hippo Pathway as Key Regulators in Stemness Maintenance, Tissue Homeostasis, and Tumorigenesis. Front Oncol 9: 60. https://doi.org/10.3389/fonc.2019.00060 PMID: 30805310

53. Kim Y, Jho EH (2018) Regulation of the Hippo signaling pathway by ubiquitin modification. BMB reports 51: 143–150. https://doi.org/10.5483/BMBRep.2018.51.3.017 PMID: 29366444

54. Ma S, Meng Z, Chen R, Guan KL (2018) The Hippo Pathway: Biology and Pathophysiology. Annual review of biochemistry https://doi.org/10.1146/annurev-biochem-013118-111829

55. Meng Z, Moroishi T, Guan KL (2016) Mechanisms of Hippo pathway regulation. Genes & development 30: 1–17.

56. Misra JR, Irvine KD (2018) The Hippo Signaling Network and Its Biological Functions. Annu Rev Genet 52: 65–87. https://doi.org/10.1146/annurev-genet-120417-031621 PMID: 30183404

57. Seo J, Kim J (2018) Regulation of Hippo signaling by actin remodeling. BMB reports 51: 151–156. https://doi.org/10.5483/BMBRep.2018.51.3.012 PMID: 29353600

58. Sudol M, Harvey KF (2010) Modularity in the Hippo signaling pathway. Trends in biochemical sciences 35: 627–633. https://doi.org/10.1016/j.tibs.2010.05.010 PMID: 20598891

59. Chan SW, Lim CJ, Guo F, Tan I, Leung T, et al. (2013) Actin-binding and cell proliferation activities of angiomotin family members are regulated by Hippo pathway-mediated phosphorylation. The Journal of biological chemistry 288: 37296–37307. https://doi.org/10.1074/jbc.M113.527598 PMID: 24225952

60. Cox CM, Mandell EK, Stewart L, Lu R, Johnson DL, et al. (2015) Endosomal regulation of contact inhibition through the AMOT:YAP pathway. Molecular biology of the cell 26: 2673–2684. https://doi.org/10.1091/mbc.E15-04-0224 PMID: 25995376

61. Hong W (2013) Angiomotin'g YAP into the nucleus for cell proliferation and cancer development. Science signaling 6: pe27.

62. Mana-Capelli S, Paramasivam M, Dutta S, McCollum D (2014) Angiomotins link F-actin architecture to Hippo pathway signaling. Molecular biology of the cell 25: 1676–1685. https://doi.org/10.1091/mbc.E13-11-0701 PMID: 24648494

63. Moleirinho S, Guerrant W, Kissil JL (2014) The Angiomotins—from discovery to function. FEBS letters 588: 2693–2703. https://doi.org/10.1016/j.febslet.2014.02.006 PMID: 24548561

64. Moleirinho S, Hoxha S, Mandati V, Curtale G, Troutman S, et al. (2017) Regulation of localization and function of the transcriptional co-activator YAP by angiomotin. eLife 6.

65. Zhao B, Li L, Lu Q, Wang LH, Liu CY, et al. (2011) Angiomotin is a novel Hippo pathway component that inhibits YAP oncoprotein. Genes & development 25: 51–63.

66. Lv M, Li S, Luo C, Zhang X, Shen Y, et al. (2016) Angiomotin promotes renal epithelial and carcinoma cell proliferation by retaining the nuclear YAP. Oncotarget 7: 12393–12403. https://doi.org/10.18632/oncotarget.7161 PMID: 26848622

67. Kim M, Kim M, Park SJ, Lee C, Lim DS (2016) Role of Angiomotin-like 2 mono-ubiquitination on YAP inhibition. EMBO reports 17: 64–78. https://doi.org/10.15252/embr.201540809 PMID: 26598551

68. Yi C, Shen Z, Stemmer-Rachamimov A, Dawany N, Troutman S, et al. (2013) The p130 isoform of angiomotin is required for Yap-mediated hepatic epithelial cell proliferation and tumorigenesis. Science signaling 6: ra77.

69. Chan SW, Lim CJ, Chong YF, Pobbati AV, Huang C, et al. (2011) Hippo pathway-independent restriction of TAZ and YAP by angiomotin. The Journal of biological chemistry 286: 7018–7026. https://doi.org/10.1074/jbc.C110.212621 PMID: 21224387

70. Sudol M, Shields DC, Farooq A (2012) Structures of YAP protein domains reveal promising targets for development of new cancer drugs. Seminars in cell & developmental biology 23: 827–833.

71. Oka T, Mazack V, Sudol M (2008) Mst2 and Lats kinases regulate apoptotic function of Yes kinase-associated protein (YAP). The Journal of biological chemistry 283: 27534–27546. https://doi.org/10.1074/jbc.M804380200 PMID: 18640976

72. Zhao B, Wei X, Li W, Udan RS, Yang Q, et al. (2007) Inactivation of YAP oncoprotein by the Hippo pathway is involved in cell contact inhibition and tissue growth control. Genes & development 21: 2747–2761.

73. Nardone G, Oliver-De La Cruz J, Vrbsky J, Martini C, Pribyl J, et al. (2017) YAP regulates cell mechanics by controlling focal adhesion assembly. Nature communications 8: 15321. https://doi.org/10.1038/ncomms15321 PMID: 28504269

74. Fan R, Kim NG, Gumbiner BM (2013) Regulation of Hippo pathway by mitogenic growth factors via phosphoinositide 3-kinase and phosphoinositide-dependent kinase-1. Proceedings of the National Academy of Sciences of the United States of America 110: 2569–2574. https://doi.org/10.1073/pnas.1216462110 PMID: 23359693

75. Plouffe SW, Lin KC, Moore JL 3rd, Tan FE, Ma S, et al. (2018) The Hippo pathway effector proteins YAP and TAZ have both distinct and overlapping functions in the cell. The Journal of biological chemistry 293: 11230–11240. https://doi.org/10.1074/jbc.RA118.002715 PMID: 29802201

76. Mana-Capelli S, McCollum D (2018) Angiomotins stimulate LATS kinase autophosphorylation and act as scaffolds that promote Hippo signaling. The Journal of biological chemistry 293: 18230–18241. https://doi.org/10.1074/jbc.RA118.004187 PMID: 30266805

77. Zaltsman Y, Masuko S, Bensen JJ, Kiessling LL (2019) Angiomotin Regulates YAP Localization during Neural Differentiation of Human Pluripotent Stem Cells. Stem Cell Reports https://doi.org/10.1016/j.stemcr.2019.03.009 PMID: 31006631

78. Shtanko O, Sakurai Y, Reyes AN, Noel R, Cintrat JC, et al. (2018) Retro-2 and its dihydroquinazolinone derivatives inhibit filovirus infection. Antiviral research 149: 154–163. https://doi.org/10.1016/j.antiviral.2017.11.016 PMID: 29175127

79. Madara JJ, Han Z, Ruthel G, Freedman BD, Harty RN (2015) The multifunctional Ebola virus VP40 matrix protein is a promising therapeutic target. Future virology 10: 537–546. https://doi.org/10.2217/fvl.15.6 PMID: 26120351

80. Garnier L, Wills JW, Verderame MF, Sudol M (1996) WW domains and retrovirus budding. Nature 381: 744–745. https://doi.org/10.1038/381744a0 PMID: 8657277

81. Han Z, Schwoerer MP, Hicks P, Liang J, Ruthel G, et al. (2018) Host Protein BAG3 is a Negative Regulator of Lassa VLP Egress. Diseases 6.

82. Liang J, Sagum CA, Bedford MT, Sidhu SS, Sudol M, et al. (2017) Chaperone-Mediated Autophagy Protein BAG3 Negatively Regulates Ebola and Marburg VP40-Mediated Egress. PLoS pathogens 13: e1006132. https://doi.org/10.1371/journal.ppat.1006132 PMID: 28076420

83. Ulbricht A, Eppler FJ, Tapia VE, van der Ven PF, Hampe N, et al. (2013) Cellular mechanotransduction relies on tension-induced and chaperone-assisted autophagy. Current biology: CB 23: 430–435. https://doi.org/10.1016/j.cub.2013.01.064 PMID: 23434281

84. Troyanovsky B, Levchenko T, Mansson G, Matvijenko O, Holmgren L (2001) Angiomotin: an angiostatin binding protein that regulates endothelial cell migration and tube formation. The Journal of cell biology 152: 1247–1254. https://doi.org/10.1083/jcb.152.6.1247 PMID: 11257124

85. Mercenne G, Alam SL, Arii J, Lalonde MS, Sundquist WI (2015) Angiomotin functions in HIV-1 assembly and budding. eLife 4.

86. Pei Z, Bai Y, Schmitt AP (2010) PIV5 M protein interaction with host protein angiomotin-like 1. Virology 397: 155–166. https://doi.org/10.1016/j.virol.2009.11.002 PMID: 19932912

87. Ray G, Schmitt PT, Schmitt AP (2019) Angiomotin-Like 1 Links Paramyxovirus M Proteins to NEDD4 Family Ubiquitin Ligases. Viruses 11.

88. Oka T, Schmitt AP, Sudol M (2012) Opposing roles of angiomotin-like-1 and zona occludens-2 on pro-apoptotic function of YAP. Oncogene 31: 128–134. https://doi.org/10.1038/onc.2011.216 PMID: 21685940

89. Adler JJ, Heller BL, Bringman LR, Ranahan WP, Cocklin RR, et al. (2013) Amot130 adapts atrophin-1 interacting protein 4 to inhibit yes-associated protein signaling and cell growth. The Journal of biological chemistry 288: 15181–15193. https://doi.org/10.1074/jbc.M112.446534 PMID: 23564455

90. Zhang C, Wang F, Xie Z, Chen L, Sinkemani A, et al. (2018) AMOT130 linking F-actin to YAP is involved in intervertebral disc degeneration. Cell Prolif 51: e12492. https://doi.org/10.1111/cpr.12492 PMID: 30039887

91. Citi S, Guerrera D, Spadaro D, Shah J (2014) Epithelial junctions and Rho family GTPases: the zonular signalosome. Small GTPases 5: 1–15.

92. Spadaro D, Tapia R, Pulimeno P, Citi S (2012) The control of gene expression and cell proliferation by the epithelial apical junctional complex. Essays in biochemistry 53: 83–93. https://doi.org/10.1042/bse0530083 PMID: 22928510

93. Yi C, Troutman S, Fera D, Stemmer-Rachamimov A, Avila JL, et al. (2011) A tight junction-associated Merlin-angiomotin complex mediates Merlin's regulation of mitogenic signaling and tumor suppressive functions. Cancer cell 19: 527–540. https://doi.org/10.1016/j.ccr.2011.02.017 PMID: 21481793

94. Zheng Y, Vertuani S, Nystrom S, Audebert S, Meijer I, et al. (2009) Angiomotin-like protein 1 controls endothelial polarity and junction stability during sprouting angiogenesis. Circulation research 105: 260–270. https://doi.org/10.1161/CIRCRESAHA.109.195156 PMID: 19590046

95. Han Z, Sagum CA, Bedford MT, Sidhu SS, Sudol M, et al. (2016) ITCH E3 Ubiquitin Ligase Interacts with Ebola Virus VP40 to Regulate Budding. Journal of virology https://doi.org/10.1128/JVI.01078-16 PMID: 27489272

96. Aragon E, Goerner N, Xi Q, Gomes T, Gao S, et al. (2012) Structural basis for the versatile interactions of Smad7 with regulator WW domains in TGF-beta Pathways. Structure 20: 1726–1736. https://doi.org/10.1016/j.str.2012.07.014 PMID: 22921829

97. Tubert-Brohman I, Sherman W, Repasky M, Beuming T (2013) Improved docking of polypeptides with Glide. Journal of chemical information and modeling 53: 1689–1699. https://doi.org/10.1021/ci400128m PMID: 23800267